

CRACK DETECTION IN SHAFT USING VIBRATION MEASUREMENTS AND
ANALYSIS

By

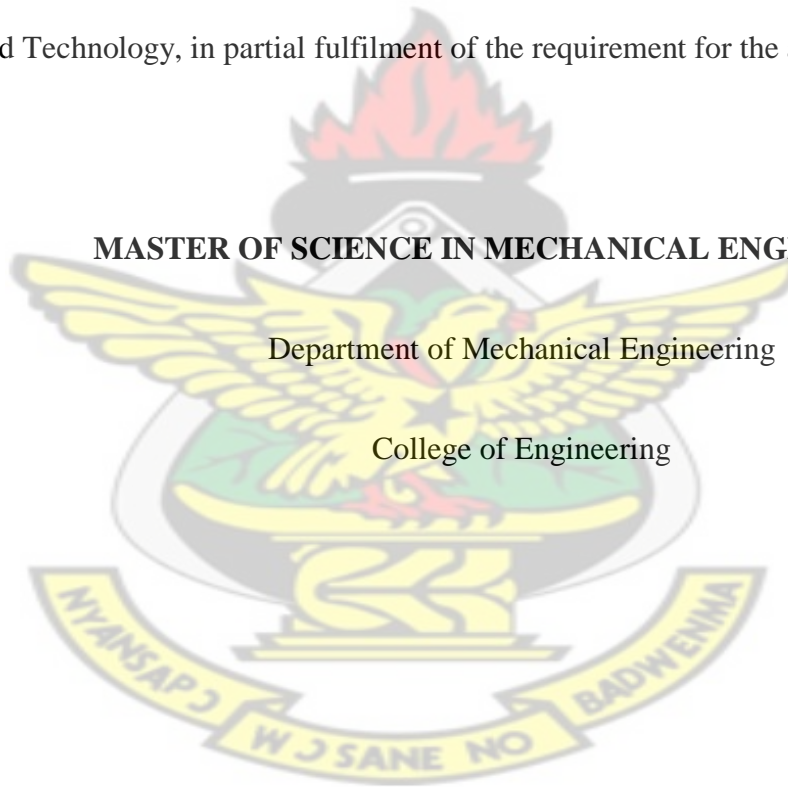
Daniel Adofo Ameyaw, BSc. Mech. Eng. (Hons.)

A Thesis submitted to the School of Graduate Studies, Kwame Nkrumah University of Science
and Technology, in partial fulfilment of the requirement for the award of the degree of

MASTER OF SCIENCE IN MECHANICAL ENGINEERING

Department of Mechanical Engineering

College of Engineering



OCTOBER, 2014

DECLARATION

I hereby declare that this submission is my own work towards the Master of Science in Mechanical Engineering and that, to the best of my knowledge, it contains no material which has been accepted for the award of any other degree of the university or any other university, except where due acknowledgement has been made in the text.

Daniel Adofo Ameyaw

(PG 7801812)

Signature

Date

Certified by:

Mr Michael Nii Sackey

(Supervisor)

Signature

Date

Department of Mechanical Engineering

KNUST.

Dr. Gabriel Takyi

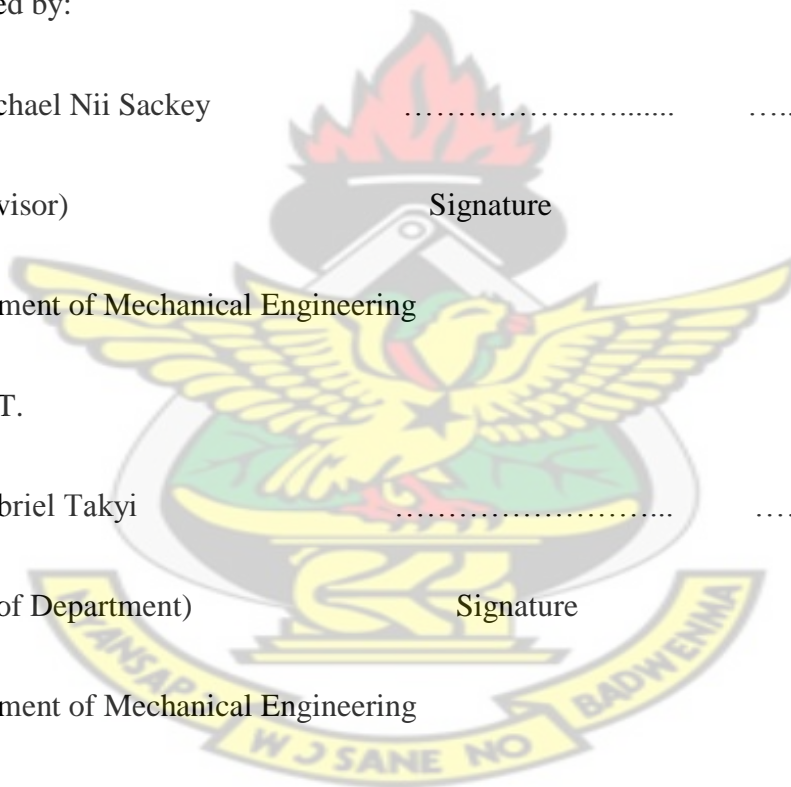
(Head of Department)

Signature

Date

Department of Mechanical Engineering

KNUST.



ACKNOWLEDGEMENT

I would like to express my sincere gratitude to my supervisors; Mr. Michael Nii Sackey, Faisal Wahib Adams and Dr. L.E. Ansong for their enormous contributions and guidance.

I would also like to extend my appreciation to Edem Dennis Dzebre, Bismark Boateng, Joseph Nyumutsu, Philip Agyeman, Kokloku Emmanuel and the entire Mechanical Engineering department, KNUST for their support.

To my family and friends, I treasure the moral support and encouragement you gave me.



Abstract

Cracks in shafts have been identified as a significant factor limiting the safe and reliable operation of machines. Cracked shafts still pose a significant and real threat to machines in spite of the great advances made in the areas of metallurgy, design and manufacturing. The ability to detect cracks at an early stage of progression is imperative to avert the aforementioned consequences which include failure of equipment resulting in costly process upsets and repairs among others. In this work, torsional and transverse vibration experiments are carried out to investigate transverse crack signatures for a shaft. The effect of the depth and position of an open transverse crack on the shaft's torsional rigidity, fundamental peak acceleration, and natural frequency was investigated. A Matlab program was also developed to aid in the computation of the natural frequency for any given crack depth and position. The program also makes it possible to calculate the deflection of the shaft mass and the masses (rotor) it carries for any given crack depth. Numerical studies were also carried out by modelling the crack using Solidworks (ver.2014) to compute the frequency. From the work, it was evident that the presence of a crack affects its modal properties and cracks at the centre posed a higher risk as compared to those at the ends. Comparing the results from the three approaches, it was observed that the analytical results were closer to that of the experimental though the numerical also gave very good results.

Table of Contents

DECLARATION	ii
ACKNOWLEDGEMENT	iii
Abstract.....	iv
List of Table	viii
List of Figures	ix
LIST OF ACRONYMS.....	xii
LIST OF NOTATION	xiii
CHAPTER 1	1
INTRODUCTION	1
1.1 Background of the study	1
1.2 Justification	2
1.3 Objective(s)	3
1.4 Scope of Work and Delimitation	4
1.5 Thesis Organisation	4
CHAPTER 2	5
LITERATURE REVIEW	5
2.1 General.....	5
2.2 Causes of shaft cracks	5
2.3 Types of shaft cracks.	7
2.4 Crack detection techniques.....	8
2.4.1 Vibration-based methods (VBM)	9
2.4.2 Modal Testing.....	18
2.4.3. Non-Traditional Methods	24
CHAPTER 3	30
MATERIALS AND METHODS	30

3.1 Torsional Vibration Experiment.....	30
3.1.1 Shaft Material Selection	30
3.1.2 Shaft specimen creation.....	32
3.1.3 Dimensions of the shaft specimen	32
3.1.4 Shaft crack shape	33
3.1.5 Generation of the crack.....	34
3.1.6 Shaft crack position and depth.....	34
3.1.7 Instrumentation for Torsional experiment.....	35
3.1.8 Torsional Vibration Experimental Work	35
3.2 Transverse Vibration Experiment.....	37
3.2.1 Shaft Material selection and Creation.....	38
3.2.2 Dimensions of the shaft specimen	38
3.2.3 Generation of crack.....	39
3.2.4 Shaft crack position and depth.....	39
3.2.5 Instrumentation for Transverse experiment	39
3.2.6 Transverse Vibration Experimental Work.....	40
4.3 Theoretical Approach.....	42
3.3.1 Analytical Approach (Dunkerley's method).....	42
4.3.2 Numerical method	46
CHAPTER 4	48
Results and Discussion	48
4.1 Torsional Vibration Results and Discussions	48
4.1.1 Results.....	48
4.1.2 Discussions	56
4.2 Transverse Vibration Results and Discussions	57
4.2.1 Results.....	57
4.2.2 Effect of crack depth and position on the natural frequency (whirling speed) of a shaft.....	64
5.1 Conclusions	68
5.2 Recommendations	69

REFERENCES..... 70

APPENDIX A..... 78

APPENDIX B..... 88

KNUST



List of Table

Table 3.1: AISI 1020 mild steel, cold drawn31

Table 3.2: Material composition of AISI 1020 mild steel, cold drawn.....31

Table 3.3: Mechanical Properties of AISI 1020 mild steel, cold drawn32

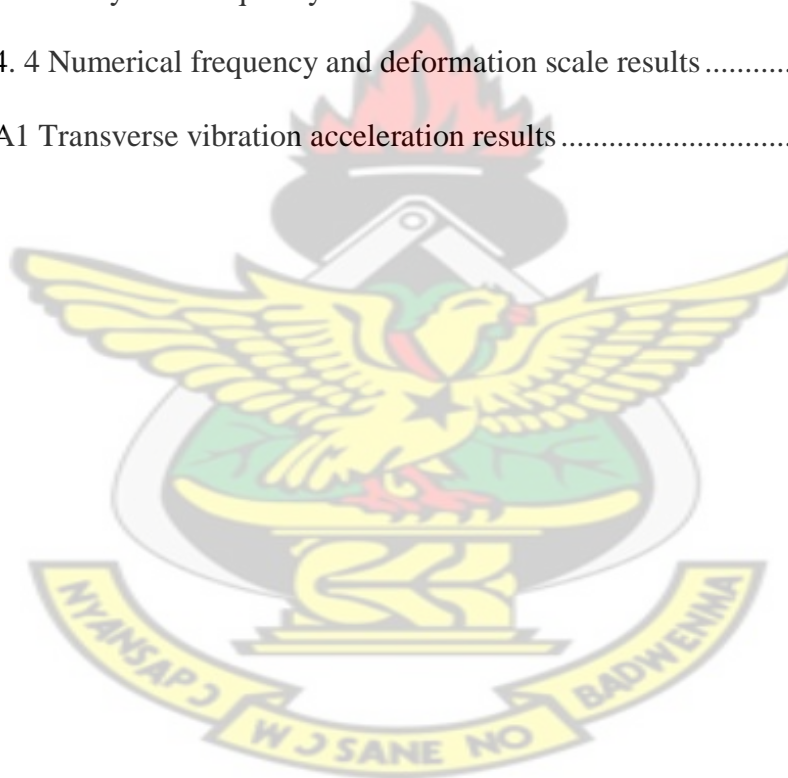
Table 4.1a: Angle of twist and corresponding Torque for different crack depths and positions.48

Table 4. 2 Experimental frequency results for different crack depths and positions64

Table 4. 3 Analytical Frequency and Deflection results65

Table 4. 4 Numerical frequency and deformation scale results66

Table A1 Transverse vibration acceleration results78



List of Figures

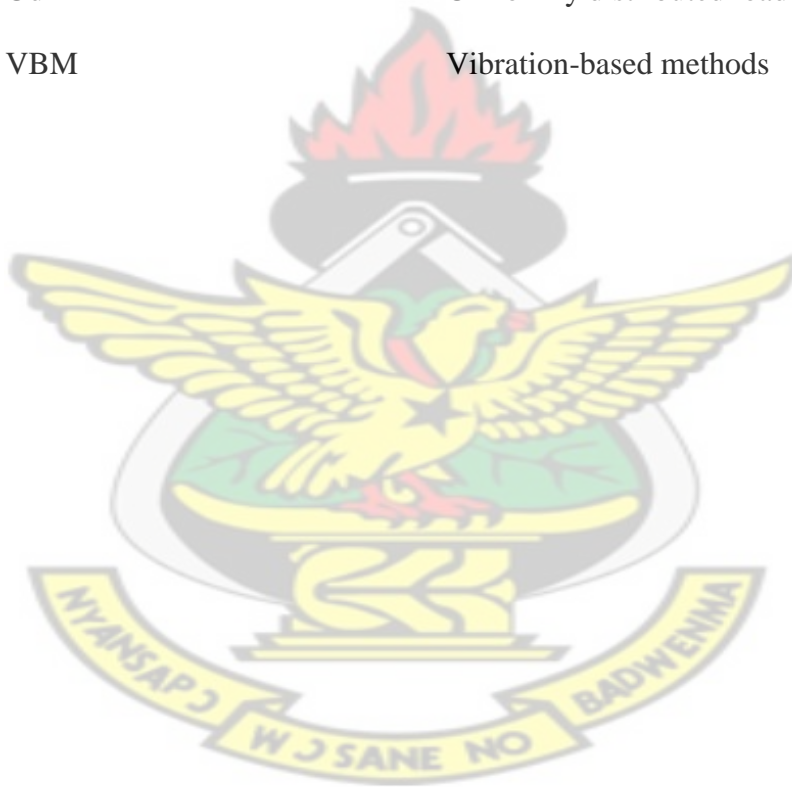
Figure 2.1: Shaft crack stimulating factors	6
Figure 2. 2: Transverse crack	7
Figure 2. 3: Longitudinal crack.....	7
Figure 2. 4: Slant crack	7
Figure 2. 5: Gaping crack.....	8
Figure 3.1: AISI 1020 mild steel shaft specimen.....	30
Figure 3. 2: Shaft specimen dimension (All dimensions in mm.....	33
Figure 3.3: V-notch crack.	33
Figure 3.4: Shaft specimen with a v-notch crack.....	34
Figure 3.5: Tecquipment SMI MKII-torsion testing machine	36
Figure 3.6: Schematic diagram showing details of torsion testing machine.....	36
Figure 3.7: Digital torque meter.....	37
Figure 3.8: Dimensions for the transverse vibration shaft specimen (All dimensions are in mm)	38
Figure 3. 9: Shaft surface crack.....	39
Figure 3. 10: Transverse vibration experimental setup.....	40
Figure 3. 11: Digital vibration meter.....	41
Figure 3. 12 Shaft with point and uniformly distributed load.....	42
Figure 3. 13 Division of cracks into sections based on the position of crack.....	43
Figure 3. 14 3-D model of the shaft	46
Figure 3. 15 Meshed shaft.....	47

Figure 4.1: Comparison between an intact shaft and a shaft with 1 mm depth at a distance of 25 mm.....	50
Figure 4.2: Comparison between an intact shaft and a shaft with 1 mm depth at a distance of 38 mm.....	50
Figure 4.3: Comparison between an intact shaft and a shaft with 1 mm depth at a distance of 51 mm.....	51
Figure 4.4: Comparison between an intact shaft and a shaft with 2 mm depth at a distance of 25 mm.....	51
Figure 4.5: Comparison between an intact shaft and a shaft with 2 mm depth at a distance of 38 mm.....	52
Figure 4.6: Comparison between an intact shaft and a shaft with 2 mm depth at a distance of 51 mm.....	52
Figure 4.7: Comparison between an intact shaft and a shaft with 3 mm depth at a distance of 25 mm.....	53
Figure 4.8: Comparison between an intact shaft and a shaft with 3 mm depth at a distance of 38 mm.....	53
Figure 4.9: Comparison between an intact shaft and a shaft with 3 mm depth at a distance of 51 mm.....	54
Figure 4.10: Comparison between three shafts with the same crack depth (1 mm) at different positions (25mm, 38mm & 51mm).....	54
Figure 4.11: Comparison between three shafts with the same crack depth (2 mm) at different positions (25mm, 38mm & 51mm).....	55
Figure 4.12: Comparison between three shafts with the same crack depth (3 mm) at different positions (25mm, 38mm & 51mm).....	55
Figure 4. 13 Acceleration spectrum for shaft with no crack	57

Figure 4. 14 Acceleration spectrum for shaft with 2.5 mm crack depth at 20 cm from left end	57
Figure 4. 15 Acceleration spectrum for shaft with 2.5 mm crack depth at centre	58
Figure 4. 16 Acceleration spectrum for shaft with 2.5 mm crack depth at 20 cm from right end	58
Figure 4. 17 Acceleration spectrum for shaft with 5.0 mm crack depth at centre	59
Figure 4. 18 Acceleration spectrum for shaft with 5.0 mm crack depth at 20 cm from right end	59
Figure 4. 19 Comparison between the acceleration spectrum of an intact shaft and a shaft with 2.5 mm crack depth at 20 cm from left end	60
Figure 4. 20 Comparison between the acceleration spectrum of an intact shaft and a shaft with 2.5 mm crack depth at centre	60
Figure 4. 21 Comparison between the acceleration spectrum of an intact shaft and a shaft with 2.5 mm crack depth at 20 cm from right end	61
Figure 4. 22 Comparison between the acceleration spectrum of an intact shaft and a shaft with 5.0 mm crack depth at 20 cm from left end	61
Figure 4. 23 Comparison between the acceleration spectrum of an intact shaft and a shaft with 5.0 mm crack depth at centre	62
Figure 4. 24 Comparison between the acceleration spectrum of an intact shaft and a shaft with 5.0 mm crack depth at 20 cm from right end	62
Figure 4. 25 Comparison between the acceleration spectrums of shafts with 2.5 mm crack depth at different positions (20cm, 36.8cm & 53.6cm).	63
Figure 4. 26 Comparison between the acceleration spectrums of shafts with 5.0 mm crack depth at different positions (20cm, 36.8cm & 53.6cm).	63

LIST OF ACRONYMS

Acronym	Meaning
AISI	American Iron and Steel Institute
ASTM	American Society for Testing and Materials
CWT	Continuous wavelet transform
DBTT	Ductile-brittle transition temperature
EPRI	Electric Power Research Institute
FEM	Finite Element Method
Udl	Uniformly distributed load
VBM	Vibration-based methods



LIST OF NOTATION

Notation	Meaning
$1x, 2x, 3x \dots nx$	First, second, third...nth harmonic
θ	Angle subtended from shaft centre to crack edge
A_c	Area of crack section taken off
a	Distance of load from left support
b	Distance of load from right support
δ	Static deflection due to point load
δ_s	Static deflection due to the mass of the shaft.
δ_{1s}	Deflection caused by shaft section 1
δ_{2s}	Deflection caused by shaft section 2
δ_{3s}	Deflection caused by shaft section 3
E	Young's modulus for the shaft material
f	Natural frequency of transverse vibration of the shaft
f_s	Natural frequency of transverse vibration
I	Second moment of area of the shaft
l	Total shaft length
r	Shaft radius
V_c	Volume of crack section taken off
W	Point load
w	Crack width

CHAPTER 1

INTRODUCTION

1.1 Background of the study

A shaft is a mechanical component for transmitting torque and rotation. It is usually used to connect other components of a drive train that cannot be connected directly due to distance or the need to allow for relative movement between them. Drive shafts are carriers of torque, thus, they are subject to torsion and shear stress. They must therefore be strong enough to bear the stress, whilst avoiding too much additional weight as that would in turn increase their inertia. Shafts are amongst components subjected to the most strenuous working conditions in industrial power transmission applications. They are also used in high-performance rotating equipment such as turboshaft engines, steam and gas turbines, high-speed compressors, generators, pumps, etc. Although quite robust and well designed, shafts in operation are usually susceptible to serious defects that develop without much apparent warning. They are principal candidates for fatigue cracks due to cyclical stresses, fluctuating nature of bending stresses, the presence of stress raisers (fillets, keyways, etc.) and possible design or manufacturing flaws (Sabnavis et al,2004).

Cracks are defined as any unintentional discontinuities in a shaft (material). Operating conditions and environmental factors can result in crack propagation and eventually lead to fatigue failure. The strength and durability of shafts may be compromised by the presence of cracks. Due to the high stress concentration in the vicinity of a crack tip it can result in the failure of the structure. Consequences of total shaft failure can be catastrophic with enormous costs in down time, consequential damage to equipment and potential injury to personnel. Total failure occurs when the specimen has completely fractured into two or more parts. A flaw or defect, in contrast, can be defined as any characteristic that renders a component less suitable for the intended use. Operators and maintenance personnel of critical plant

machinery are particularly interested in early detection of symptoms that can lead to in-service failure of shafts. In shafts, cracks are initiated as tiny discontinuities that grow in size when the component is subjected to cyclic stresses. Early detection of crack becomes necessary before it gets to the critical size and cause total shaft failure.

1.2 Justification

Despite the advances made in the production of shafts, through improvements in manufacturing methods and design capabilities, shaft cracks still pose a significant threat to its operation. Although, usually quite robust and well designed, serious defects can develop in shafts without much apparent warning. Total shaft failure can be catastrophic as it can lead to injury and even death in extreme situations. There are a few types of shaft cracks which can develop during the operation of rotating machines. The transverse crack remains the most critical type of crack as the machine safety is significantly influenced by its occurrence.

Although clear statistics are not available as to the extent of damage caused by cracked shafts, the Electric Power Research Institute (EPRI) estimates direct and indirect losses (repair, replacement and loss of revenue) at around US \$1 billion in the conventional and nuclear power industry alone (Sabnavis et al,2004). Cases range from catastrophic rotor bursts to detection of cracks at a much later stage, resulting in repair or retirement of the shaft. In Ghana, there are no clear statistics detailing the incidents of shaft cracks in industries as well as the cost of these incidences on the economy, but the detection of a crack on the rotor of one of the steam turbines at the Takoradi Thermal Power Plant at an advanced stage was fatal. It has therefore become imperative to investigate crack signatures to serve as a diagnostic tool for online condition monitoring purposes.

Though some works have looked at transverse cracks, more emphasis was placed on the crack depth neglecting the crack position. It is therefore necessary to explore the effect of crack depth and position on a shaft's static and dynamic behaviour. It is also necessary to model numerically and analytically develop a program that can compute the changes in a shafts natural frequency as a result of the presence of a crack.

1.3 Objective(s)

The main objective of this work is to study the effects of crack depth and position on the static and dynamic behaviour of a shaft, as well as to simulate and develop a program that can compute the natural frequency of an intact and defective (cracked) shaft.

Specific objectives are:

- i. Conduct a detailed review of the literature relating to detection techniques for cracked shafts in machinery.
- ii. Experimentation to establish signatures of a healthy and a defective (cracked) shaft.
- iii. Investigate the effects of the size and position of a crack on a shaft.
- iv. Write an Algorithm to be able to compute the natural frequency and deflection of an intact and defective shaft.
- v. Simulate the crack using the FEM package in Solidworks (ver.2014) and compute the natural frequency.

1.4 Scope of Work and Delimitation

The scope of this work was limited to experiments carried out on shaft specimen in the laboratory. Torsional and transverse vibration experiments were carried out on a healthy and defective (cracked) shaft specimen to determine its static and dynamic behaviour. Matlab programming was used to develop a programme that could compute the natural frequency and deflection of the shaft. The crack was also modelled using Solidworks (ver.21014) and the natural frequency and deformation scale computed numerically.

1.5 Thesis Organisation

Chapter 1 describes what the whole thesis is about, thus, it gives a general description of what would be expected in this work. It begins with giving background information of the work, followed by what necessitated the choice of the thesis topic, the objectives, as well as the scope and limitation of the work. Chapter 2 presents a detailed review of the literature relating to detection techniques for cracked shafts in rotating machinery. The detection techniques are grouped into three main categories: (1) vibration-based methods; (2) modal testing; (3) non-traditional methods. The methodology used is presented in the next chapter. The materials used, the experimental procedure as well as the instruments used, are all presented in chapter 3. Detailed experimental results and discussions are outlined in chapter 4, where the data obtained from the experiments are analysed. Chapter 5 presents the conclusion and recommendations for future works.

CHAPTER 2 LITERATURE REVIEW

2.1 General

In the most general terms, cracks can be defined as changes appearing in a shaft (material) that may affect its current or future performance. From this definition, it can be adduced that, the definition of crack is not meaningful without a comparison between two different states of the specimen, one of which represents the initial (intact) state, and the other the defective (cracked) state.

2.2 Causes of shaft cracks

Current trends in rotating machinery design and operation result in severe stress imposed on rotors. High mechanical stress results from the general trend to increase the power of machines which is associated with the rotative motion of shafts. A typical chronology of events leading to total failure by cracking in a ductile material, as per Bloch (1997) and Fuchs and Stephens (2000) is as follows.

Crack initiation: Tiny discontinuities are initiated in the uncracked parent material at this stage. Cracks may be caused by mechanical stress raisers, such as sharp keyways, abrupt cross-sectional changes, heavy shrink fits, dents and grooves, or factors such as fretting and/or metallurgical factors such as forging flaws, inclusions, porosity and voids.

Crack propagation: During this stage, the discontinuity grows in size as a result of the cyclic stresses induced in the component. Certain conditions, some of which are listed below, can accelerate the crack growth rate:

- I. Operating faults, such as sustained surging in compressors, negative sequence current or grounding faults in generators and coupled turbines.

- II. The presence of residual stresses or welding heat affected zones (HAZs) in the rotor material.
- III. Thermal stresses.
- IV. Metallurgical conditions, such as the presence of hydrogen in steel, elevated ductile–brittle transition temperature (DBTT), carbide precipitation in alloy steels.
- V. Environmental conditions such as the presence of a corrosive medium.

The actual failure of the material can be in a brittle or ductile mode, depending on the prevailing conditions. Failure occurs very rapidly once the crack reaches a critical size.

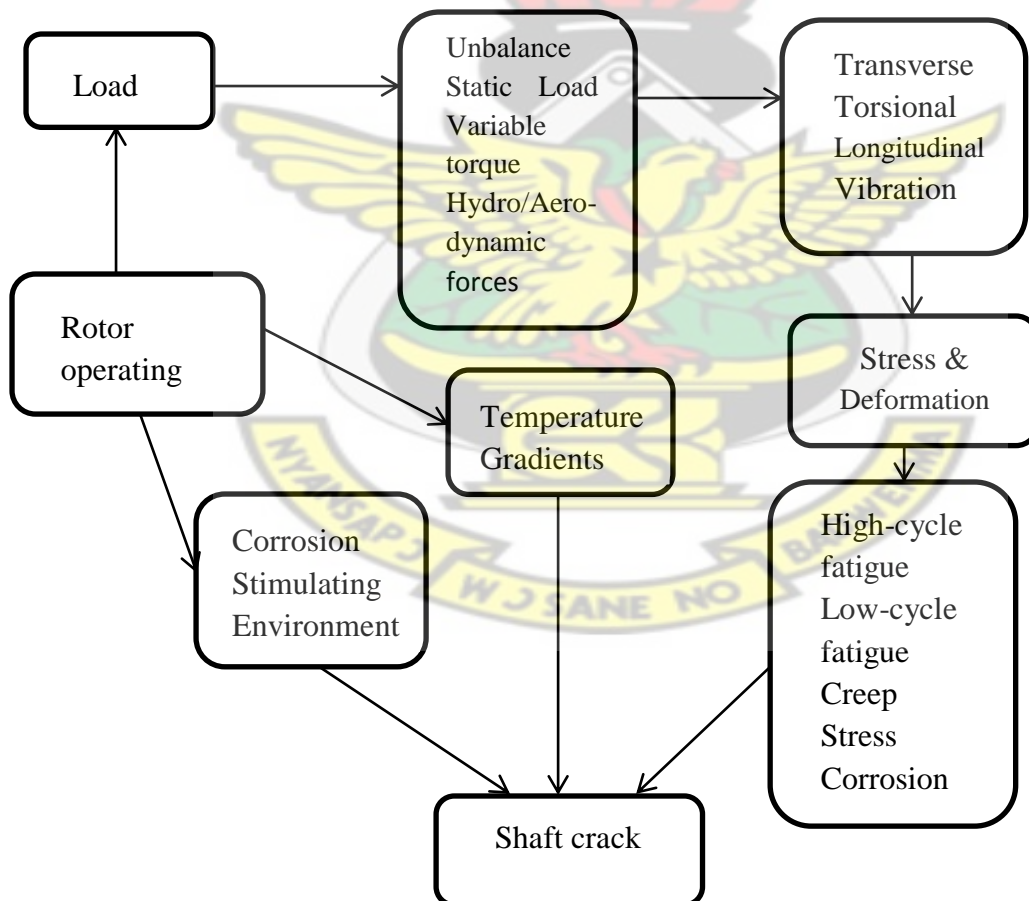


Figure 2.1: Shaft crack stimulating factors

2.3 Types of shaft cracks.

Based on their geometries, cracks can be broadly classified as follows;

- i. Cracks perpendicular to the shaft axis are known as “transverse” cracks. These are the most common and most serious as they reduce the cross-section and thereby weaken the rotor. Most past and current research focuses on the detection of such cracks. They introduce a local flexibility in the stiffness of the shaft due to strain energy concentration in the vicinity of the crack tip.



Figure 2. 2 Transverse crack

- ii. Cracks parallel to the shaft axis are known as “longitudinal” cracks.



Figure 2. 3 Longitudinal crack

- iii. “Slant” cracks (cracks at an angle to the shaft axis) are also encountered, but not very frequently. Slant cracks influence the torsional behaviour of the rotor in a manner quite similar to the effect of transverse cracks on the lateral behaviour. Their effect on lateral vibrations is less than that of transverse cracks of comparable severity (Ichimonji et al, 1994 and sekhar, 1999).



Figure 2. 4 Slant crack

- iv. Cracks that open when the affected part of the material is subjected to tensile stresses and close when the stress is reversed are known as “breathing” cracks. The stiffness of the component is most influenced when under tension. The “breathing” of the crack results in non-linearities in the vibrational behaviour of the rotor. Shaft cracks breath when crack sizes are small, running speeds are low and radial forces are large (Sekhar and Prabhu, 1998). Most theoretical research efforts are concentrated on “transverse breathing” cracks due to their direct practical relevance.
- v. Cracks that always remain open are known as “gaping” cracks. They are more correctly called “notches”. Gaping cracks are easy to mimic in a laboratory environment and hence most experimental work is focused on this particular crack type.



Figure 2. 5 Gaping crack

- vi. Cracks that open on the surface are called “surface” cracks. They can normally be detected by techniques such as dye-penetrant or visual inspection.
- vii. Cracks that do not show on the surface are called “subsurface” cracks. Special techniques such as ultrasonic, magnetic particle, radiography or shaft voltage drop are needed to detect them. Surface cracks have a greater effect than subsurface cracks on the vibrational behaviour of shafts (Subbiah et al., 2002).

2.4 Crack detection techniques

The reviewed literature is broadly grouped into three categories;

1. Vibration-based methods(VBM),

2. Modal testing,
3. Non-traditional methods.

2.4.1 Vibration-based methods (VBM)

The vibration based methods of crack detection can further be divided into two main categories namely;

- i. Signal based methods; which employs vibration monitoring equipment such as accelerometer's, eddy-current transducers, proximity probes, spectrum analysers, among others.
- ii. Model based methods; that are based on analytical or numerical models to simulate the behaviour of cracked shafts during operation and attempts to correlate the observed vibration signature with the presence of a crack at discrete locations on the shaft.

Several works (Bently and Muszynska, 1986a; Allen and Bohanick, 1990; Eisenmann, 2000) have been published by researchers on case histories of detection of shaft cracks using signal-based methods. In several cases, fretting corrosion, misalignment and heavy side loads have been identified as the causes for shaft cracks in compressors, generators, gears and nuclear coolant pumps. With regards to the VBM technique for crack detection, Bently and Muszynska (1986a) are of the opinion that changes in shaft position and steadily increasing 1x component trends at steady state are reliable indicators. Bearing housing measurements are not as reliable as direct shaft measurements. Although several other researchers have found the 2x component to be a good indicator of shaft cracks, Werner (1993) is also of the opinion that the trend of the 1x component is a better indicator. The 2x component in the signature of a cracked shaft is primarily because of the local asymmetric shaft stiffness (due to a crack) and the presence of radial loads. The 2x component is too sensitive to other factors

such as side loads, misalignment, support system asymmetry, etc., to be a reliable indicator of shaft cracks.

Several other authors recommend observing the shaft $2x$ component. Saavedra and Cuitino (2002) present a theoretical and experimental analysis to demonstrate that the $2x$ component of vibration for horizontal shafts at half the first critical speed value is a good indicator. Based on their study of fracture mechanics, Lazzeri et al. (1992) also suggest that monitoring the $2x$ component during the operation of a machine helps to identify cracks. It is also mentioned that observing the $2x$ component during start-up/coast-down is more useful than during steady-state operation (Bently and Muszynska, 1986b). Sanderson (1992) describes the detection of a propagating crack in a 935 MW turbo-generator in a nuclear plant soon after commissioning. The depth of the crack reached 25% of the shaft diameter before its presence could be confirmed and the machine was taken out of service. Factors that helped identify the crack were as follows:

- (a) a large and steadily increasing $1x$ component due to shaft crack induced unbalance, the temperature gradient within the rotor was quite large from bore to surface, and the crack distorted the distribution of thermal stresses, which resulted in bending of the shaft;
- (b) a small reduction in generator first and second critical speeds observed during run up;
- (c) large $2x$ component at half the generator first critical speed;
- (d) split first critical speed due to asymmetry in the normally symmetrical rotor (four-pole generator).

Muszynska et al. (1992) state that torsional vibrations are excited even by purely radial forces, such as unbalance and misalignment in the case of cracked shafts. Thus, monitoring

the torsional vibrations in many horizontal and vertical machines, when $8x$, $6x$, $4x$ etc. of speeds correspond to the lowest torsional frequency, can help to detect cracks. Torsional vibrations are seldom monitored in turbomachinery for a variety of reasons including the complexity involved and the prevalent idea in the industry that they are not of great importance. The authors also feel that, with improvements in transducer and signal conditioning technology, torsional vibration monitoring of turbomachines will increase in application.

Dorfman and Trubelja (1999) exhaustively cover the subject of torsional vibrations in steam turbines and turbo-generators and its application in crack detection. They address the instrumentation, data acquisition and signal processing aspects of monitoring torsional vibrations. They also cover the common problems encountered during the above steps and their remedies.

Ishida et al. (1995) suggest an alternative indicator for detecting cracks in rotors operating in the transcritical and supercritical ranges. Instead of monitoring $1x$ or $2x$ components, they suggest that, in the $2\omega_c/3$ to $2\omega_c$ range, the $1/2x$, $3/2x$ and $9/2x$ components should be monitored as they are most sensitive to cracks (where ω_c is the critical speed of the rotor). Gasch and Liao (1996) have patented an orbit-based method of crack detection. The shaft vibration signal is decomposed into forward and backward orbits of $1x$, $2x$ and $3x$ frequencies. The inventors are of the opinion that continuous monitoring of the backward harmonics, especially during transients, can reveal the presence of cracks. Experimental verification of the above method is demonstrated on a variable crack depth rig in Liao and Gasch (1992). Plaut et al. (1994) investigate the transient behaviour of a cracked shaft during constant acceleration or deceleration past a critical- speed. Both breathing and gaping cracks are studied. The effects of acceleration rates, crack depth, eccentricity, etc., are considered.

They conclude that the response is minimized by rapid acceleration or deceleration through the critical speed zone and the response increases with an increase in crack depth. They also observe that the maximum transient response is very sensitive to the position of the unbalance vis-à-vis the crack. This phenomenon is applied to crack detection by Kavarana and Kirk (1995). They constructed a test rig wherein known unbalance weights are placed at different angles with respect to a crack and the response is measured. It is observed that the response is highest when the unbalance leads the crack by 90° . Based on analytical studies on a Laval rotor with a small transverse breathing crack,

Sekhar and Prabhu (1998) state that during run-up, the vibration response of a cracked rotor is maximum when the angle between the crack and the unbalance is 0° or 180° . They studied the effects of acceleration rate, crack depth and position of unbalance on the vibrational behaviour of a cracked rotor during run up. Additionally, they are of the opinion that the increase in the $1/2$ and $1/3$ critical response is a reliable indicator of cracks.

Several researchers have presented their work on model-based methods. Bachschmid et al. (2000a, 2000b) present a robust method for detecting the position and the depth of cracks on rotors. A model-based diagnostic approach and a least-squares identification method in the frequency domain are used for the crack localization along the rotor. The crack depth is calculated by comparing the static bending moment due to the rotor weight and the bearing alignment conditions, to the identified “equivalent” periodical bending moment, which simulates the crack. Goldman et al. (1999) analysed numerically the dynamic response of a Jeffcott rotor with small cracks, and they drew several conclusions.

Cracks can be detected by observing the non-synchronous response for running to first critical speed ratios of a half, a third and a quarter. Additionally, rotor cracks cause backward whirl at all frequencies ($1x$, $2x$, $3x$, $4x$, etc.) and each component is elliptical in shape. The

ellipticity of response orbits and variations in phase angle of responses of a cracked rotor with respect to the non-cracked one, especially in the direction of gravity, increases with crack depth. However, in the supercritical range, these particular components are relatively insignificant. The authors state that all the above rules are only valid in the stable operating region for small vibrations.

Guo et al. (2003) have applied the finite element method (FEM) to study the influence of cracks on all three types of shaft vibrations: torsional, axial and lateral. A full 12×12 stiffness matrix is considered for the crack. They state that torsional vibrations by themselves are not the most reliable indicators of shaft cracks because of their relatively small magnitudes. Instead, the presence of strong $1x$ axial vibrations on the application of purely radial excitations is a better indicator of cracking. Breathing cracks additionally produce $2x$ and $3x$ components in the lateral vibrations. Mohiuddin and Khulief (2002) present yet another FEM-based crack detection scheme. Mathematical models of the rotor are evolved and the equations of motion are solved using various techniques (reduced-order modal transformations, Hamilton, etc.). Park (1996) discusses a non-linear state observer designed to detect cracks in shafts. Using the elementary observer, an estimator (observer) bank is established and arranged at certain locations on the shaft. When a crack is detected at a particular location, the depth estimation procedure is applied. Ostachowicz and Krawczuk (1992) present a mathematical model for the stiffness of a section of shaft containing a gaping transverse crack. They derive a 5×5 flexibility matrix. The stiffness matrix is derived from fracture mechanics using stress intensity factors due to the crack, and it can be seen that the stiffness matrix has coupled terms. Hence it can be concluded that torsional and bending vibrations are coupled. The mass matrix is assumed to be unaffected by the crack. This element can be used in the FE analysis of rotors of any complexity and the behaviour can be predicted at any location and any speed. Ratan et al. (1996) define a vector quantity, called

the “residue” (Baruh and Ratan, 1993, for additional details pertaining to the residue), which is calculated from the measured vibration response of a rotor and the modeled system matrices. A non-zero value of the quantity at any section indicates the presence of a crack. This method was shown to be capable of detecting and locating cracks as small as 4% of the shaft diameter. Yang et al. (2001) study the dynamic characteristics of cracked shaft in the subcritical, transcritical and supercritical regions. The holo-spectral method is used to study the transient vibrations of the rotor. Because of the extreme sensitiveness of this technique, the authors claim that it can be applied to detect incipient cracks, i.e. even before actual cracks appear. Green and Casey (2003) present two theoretical analysis techniques. Using the global and local asymmetry models, they set about identifying the most suitable target characteristic for crack detection. The $2x$ component is shown to be the primary response component. Also, the $2x$ resonance speed is lowered due to a crack. This is especially useful during run-up or coast-down.

Meng and Hanh (1994) consider time-dependent terms as external excitation forces and analyze, both theoretically and numerically, the approximate dynamic response of a cracked horizontal rotor. For each steady-state harmonic component, the forward and backward whirl amplitudes, the shape and orientation of the elliptical orbit and the amplitude and phase of the response signals are analyzed, taking into account the effect of crack size, crack location, rotor speed and imbalance. It is found that the crack causes backward whirl, the amplitude of which increases with the crack. The influence of the crack on the synchronous response of the system can be regarded as an additional imbalance.

Depending on the speed and the crack location, the response amplitude differs from that of the uncracked rotor. The nonsynchronous response provides evidence of crack in the subcritical range but it is too small to be detected in the supercritical range. Possibilities for

crack detection over the full speed range include the additional average (the constant) response component, the backward whirl of the response, the ellipticity of the orbit, the angle between the major axis and the vertical axis and the phase angle difference between vertical and horizontal vibration signals.

Chan and Lai (1995) discuss the FE-based simulation of a shaft with a transverse crack. They analyze the four possible cases: (i) uncracked symmetrical shaft; (ii) cracked symmetrical shaft; (iii) uncracked asymmetrical shaft; (iv) cracked asymmetrical shaft. They state that the response of (ii) is very similar to that of (iii). Both show resonance at half the value of the first critical speed. However, (ii) also shows resonance at third the critical speed which (iii) does not. Also, (ii) and (iv) differ in that at half the critical speed, the 2x vibrations are much larger than the 1x in the case of (iv). This can be used as a reliable indicator for detecting shaft cracks in symmetric rotors.

Most turbomachine rotors are supported on hydrodynamic bearings. Prabhu and Sekhar (1995) present a severity estimation criterion and crack growth monitoring method for cracked shafts in fluid film bearings. The peak dynamic pressure on the oil film is used as the target criterion. As crack depth increases, the dynamic pressure also increases. It is acknowledged that the peak pressure measurements are not the best indicators because of the difficulty involved in their estimations and also because of their relative insensitivity. Various bearings were tested and it was observed that the tilting pad bearings are least sensitive to increased dynamic pressure due to cracks while three-lobe bearings are the most sensitive. Guang and Gasch (1993) investigate the stability of a cracked rotor supported on two axial groove, four lobe and five tilting pad type journal bearings. It is found that, regardless of the bearing type used, the rotor is always unstable in a certain range of speeds. For large values of the gravity factor (a measure of elasticity of shaft) the stability depends on the stiffness

ratio (along the strong and weak axes), while for smaller values it depends on the mass ratio (the ratio of lumped mass at the bearing to that at the center of the shaft). In this range, the shaft is not unstable due to the crack and its stability depends only on the bearing type and operating conditions.

Sekhar (2000) presents a unique crack detection methodology based on the measurement of the Q factor of a rotor during coast down. The Q factor is defined as the amplification factor of any selected frequency component as determined from the corresponding Bodé plot by the popular “half-power” method. Sekhar feels that this parameter, especially for the 2x component, is the most sensitive to shaft asymmetry (i.e. cracks) and sudden changes of the Q factor during coast-down are good indicators for cracks.

Soeffker et al. (1993a) apply the theory of Lyapunov exponents for non-smooth dynamical systems for cracked shaft detection. Analysis reveals the presence of chaotic motion and strange attractors in the case of a cracked rotor. To detect a crack and establish a clear relation between shaft cracks in rotors and induced phenomena in shaft vibrations measured at bearings, a model-based method is applied.

Based on a fictitious model of the time behaviour of system non-linearity, a state observer of an extended dynamical system is designed to estimate them. The theory is extended in Soeffker et al. (1993b). A new concept is presented, based on the theory of disturbance rejection control, and further extended for non-linear systems. Simulations have been carried out showing the theoretical success of this method, especially for reconstructing exciting forces as inner forces caused by the crack. Calculating the relative crack compliance as the ratio of additional compliance caused by the crack and undamaged compliance a clear relation between the opening and closing, and therefore for the existence of the crack, and also about the crack depth is possible. Theoretically, it has been shown that it is possible to

detect a crack of a depth of 5% of the radius of the rotor corresponding to very small stiffness changes. Brandon (2000) presents a review of literature on non-linear vibrations of cracked structures. The assumption of linearity of cracked structures by many researchers results in inaccurate conclusions while oversimplification or case specific study is necessary in non-linear analysis for computational reasons. Structures with flaws exhibit a unique “forced-free” behaviour because of the non-linearity that makes the detection of flaws easier. Among topics discussed in the paper are linear methods and their limitations, generation of models and assembling them for non-linear analysis. The latter aspect is of special importance because of the many subtleties involved in modelling a crack, e.g. the fact that the crack is “switching” in the case of a rotor while not in a beam, the impact closure of cracks, and the interaction between faces of closed cracks leading to an increase of effective stiffness. The paper also deals with crack detection methods based on non-linear vibrations, e.g. using the time history of signals, Poincaré plots, etc. In another paper, Roberts and Brandon (2003) present the application of transient, non-linear vibration signatures to distinguish between various possible causes of malfunction of turbomachinery. They attempt to apply the principle in diagnostics of a large hydro-generator. The occurrence of aliasing when sampling vibration data has prevented accurate differentiation between causes. This stresses the importance of proper data collection, the absence of which can lead to faulty conclusions.

Subbiah et al. (2002) present an interesting paper, although not directly related to detecting shaft cracks. They talk about the effect of torsion on shaft cracks and crack growth rates. Almost all of the published work on cracks exclusively addresses the effect of bending moment on cracks. Subbiah et al. used axi-harmonic, eight-node elements available in commercial finite element analysis (FEA) software to model a transverse shaft crack. A frame-by-frame displacement and strain energy studies were conducted. The method developed can be applied to surface and subsurface cracks. They analysed different cases

with various crack lengths subjected to bending and torsion. Based on the study, they made the following observations: (a) transverse cracks primarily respond to bending, but can also respond to torsion depending on their position; (b) surface cracks have a greater and earlier effect than subsurface cracks.

Varè and Andrieux (2001) present a paper to better understand the behaviour of cracked shafts. They state that most cases in the open literature pertain to oversimplified cases almost unsuitable for real-life application. Temperature and multicrack effects need three-dimensional, FE-based methods. They briefly mention that the most important things in the simulation of cracked shafts are the correct modelling of the local flexibility due to the crack and the “switching” effect due to shaft rotation (whereby the breathing characteristic is introduced). They attempt to develop a methodology to model and simulate cracks and implement it in the code ASTER developed by Electricité de France (EDF).

2.4.2 Modal Testing

Among the non-VBM methods available, modal testing is the most popular. Changes in system modal characteristics such as;

- Changes in mode shapes,
- Changes in system natural frequencies,
- Response to specially applied excitation (other than unbalance).

Most modal methods need the rotor to be stationary while some require the rotor to be running at a fraction of its operating speed. All the following methods were proposed after numerical or analytical studies on mathematical models and, in some cases, subsequent experimental verification on either test rigs or full-scale rotors is also carried out.

Several researchers have identified that a coupling mechanism exists between different types of vibrations, i.e. axial, radial and torsional, in cracked shafts. They recommend employing this phenomenon to identify cracks. Collins et al. (1991) investigate the excitation of a rotating, cracked shaft by single and periodic compressive axial impulses applied at one end. When periodic impulses were applied, it was observed that the vertical motion (perpendicular to the shaft axis) in non-cracked shafts decayed with time and the vibration spectrum had a single frequency component, Ω (where Ω is the rotational frequency and ωt is the frequency of application of the axial impulses). In the case of a cracked shaft, the vertical motion does not decay and the frequency spectra revealed, besides the exciting frequency (ωt), additional ($\omega t - \Omega$) and ($\omega t + \Omega$) components. Gounaris and Papadopoulos (2002) present a method wherein radial excitations are applied at one end of a rotating cracked shaft and the axial displacements are measured at the other end. Theoretical analysis is carried out for a Timoshenko shaft with a transverse gaping crack, which is modelled using a local compliance matrix. Three sets of excitation frequencies and shaft rotational speeds are needed for each case. Special contour plots are developed theoretically for each rotor-bearing system. If the axial response is measured at each run, the axial location and depth of a crack can be determined graphically from the pre developed contours. Dimarogonas and Papadopoulos (1988, 1992) and Papadopoulos and Dimarogonas (1989, 1990) have used a previously developed 6×6 flexibility matrix for a gaping transverse crack and identify coupling between bending, torsional and axial vibrations. Analysis is performed on a Timoshenko beam, with a gaping crack and hence no non-linearities were considered. Additionally, Papadopoulos and Dimarogonas (1989) also talk about the application of theory to detecting crack in a steam turbine rotor. Goldman and Muszynska (1992) dealt with the observed response of a cracked rotor system to synchronous and asynchronous radial and torsional

excitations. Torsional excitations are applied to a motor-driven experimental cracked rotor by means of a generator fed with varying excitation currents.

Lateral excitations are applied by a constant force perturbator. The reduction of shaft system torsional stiffness (due to the crack) could be identified. Experimental results are compared to the analytical model consisting of a set of non-linear equations subjected to small-order perturbations. The following conclusions were made. Reverse components, if present in the shaft vibrations, can be safely ignored and only forward components need to be considered as they have a direct relation with the shaft crack. The effect of cracks on lateral and torsional mode shapes has been confirmed but not quantified.

Ishida et al. (2001) present a theoretical study on the detection of cracks by exciting the rotor by sinusoidal asynchronous radial forces. The behaviour of the cracked shaft has been approximated by both a piecewise linear model and a power series model. It is established that, if the shaft were cracked, the following additional resonances would be observed in the vibration spectrum: $\pm (\Omega - \omega t) = (\Omega + \omega t) =$ forward and backward resonance frequencies (Ω and ωt same as above).

Iwatsubo et al. (1992) present an analytical, numerical and experimental treatment of the response of a cracked shaft to periodic exciting forces. Additionally, they also theoretically investigate the response to a radial impulse. A very good correlation is demonstrated between expected frequency components in the spectrum and observed components. In all the above papers, the speed of rotation of the shafts during excitation was kept low and also different from the system natural frequencies to minimize the effects of shaft unbalance. Sundermeyer and Weaver (1995) apply the weakly nonlinear characteristic of a cracked beam to determine the location, depth and opening load of a transverse crack. Their study is based on the simpler case of a single-degree-of-freedom system with a bilinear spring. Because of the non-

linearity, when the system is excited by two harmonic forces of different frequencies, the response has an additional frequency component, equal to the difference between the frequencies of the two exciting forces. This component is especially high when the difference corresponds to a natural frequency of the beam. A parametric study is carried out to determine the effect of crack depth, location and static load on the crack signature. Once complete charts are developed from the parametric study, determining details becomes an inverse problem that can be solved.

Prabhakar et al. (2001) present a FEM-based study on the influence of gaping and breathing cracks on the mechanical impedance of a rotor-bearing system. Impedance is defined as the ratio of the magnitude of an exciting force to the velocity response. An impulse is applied at various locations on a rotating shaft and the impedance is measured. It has been observed that the impedance at certain key frequencies reduces significantly with increase in crack depth. These key frequencies are the natural and rotor running frequencies. A breathing crack is more sensitive to impedance change than a gaping crack. Thus, Prabhakar et al. feel that systematic impedance measurement is an effective method of crack detection. Thibault et al. (1996) have patented a collar attachment that facilitates modal testing of large shafts. Radial, torsional, and other exciters can be mounted on the collar. They can be fixed at any angular position without turning the massive shaft. The same can be done with vibration measurement transducers. The remaining papers and patents deal with the effect of cracks on rotor natural frequencies and mode shapes. Goldman et al. (1996) examine the synchronous response of a cracked multimodal rotor during transient processes such as start-ups or shutdowns. A transverse crack on the rotor is treated as a structural singularity. Additional local flexibility and mass reduction are added at the crack location. The synchronous component of the modified rotor lateral response is investigated from the mode shape standpoint. Results are formulated as suggestions for improvements in vibrational diagnostics

strategy. Hamidi et al. (1992) have developed two mathematical models to study the changes in the natural frequencies due to changes in the rotor structural parameters. Transverse cracks are modelled as a local flexibility in the shaft. Mathematical models of stationary beams are verified experimentally and extended to analyse rotating beams. Based on the study, they conclude that the rate of change of natural frequency becomes rapid when crack depth exceeds about 30% of the shaft radius. It is also verified that the change in natural frequency does not depend on the speed of rotation in case of rotating beams. Torres (1996) describes a similar torsional vibration based approach towards crack detection. Torsional natural frequencies of a motor driven system (pump, compressor) are determined by measuring the three-phase current drawn by the motor. The observed frequencies are then compared to a table of natural frequencies for various crack locations and depths obtained by an exhaustive FE study of the system.

Lee and Kwon (2000) apply directional frequency response function (dFRF) testing to detect asymmetry or angle dependency in shaft stiffness. This method, although better suited for symmetric rotors, can be applied with some modification to originally asymmetric rotors. The magnitude and phase of the dFRF indicates the severity and circumferential location of a crack. This method can be performed online and uses only one exciter and one sensor. Lees (2000) discusses general vibration-based detection methods and several case studies in one paper. In addition to shaft cracks, a variety of other common malfunctions such as rubs, shaft bending, misalignment and imbalance are discussed. The dynamics of a horizontally mounted, asymmetric shaft with a transverse crack are discussed in another paper by Lees and Friswell (1999). The study is of practical importance as many machines, such as two-pole turbo-generators, etc., have inherently asymmetric rotors and still need to be diagnosed for cracks. Simulations are performed for the response of this structure for free-free and pinned modes. It is shown that, as the orientation of the rotor is varied, complicated patterns (of

responses) emerge due to the opening and closing of the crack. This is due to the rotation of the shaft's principal axes. It is shown how this may be successfully modelled to establish a consistent representation of crack behaviour. This model is then used to locate the crack and to give an estimate of its magnitude and dynamic behaviour. Munoz et al. (1997) present an off-line method for crack detection. Modal test are to be carried out on a free-free supported rotor and any unexpected change in rotor normal frequencies as measured at different angles indicates the presence of cracks. Munoz et al. claim that this method can be applied to detect cracks of areas greater than 2.5% of the rotor cross-sectional area. Tsai and Wang (1996) have developed a method which monitors the change in the natural frequencies and the mode shapes of a cracked shaft and thereby helps determine the size and location of the crack. Yen and Herman Shen (1997) investigate the effect of a transverse crack on the torsional vibration of shafts. A generalized variational principle is used to formulate the equations of motion and associated boundary conditions for the free vibration of a non-rotating cracked shaft. The natural response of the free-free shaft is then calculated through a Galerkin procedure. The results indicate a clear change in the natural frequencies of the cracked nonrotating shaft as compared to a non-cracked shaft. Zakhezin and Malysheva (2001) discuss a FE-based crack detection scheme. The rotor is carefully modelled to include system damping, etc., and the system natural frequencies are calculated. A simple rotor with and without cracks of varying depth and location was taken as an example. Over 600 eigenvectors and eigenvalues have been computed up to a frequency of 1100 Hz for the various models (with and without cracks). The modal contribution of each eigenvalue has been evaluated for stresses in elements of the model. The modes with highest stresses have been selected as the target modes for observation and comparisons. Modal tests are carried out on the actual rotor and the previously identified modes are monitored for changes. The popularity of the above methods can be judged from the large number of patents. Miller et al. (1990, 1992) and

Brook et al. (1991) describe crack detection methods that observe changes in natural frequencies, mode shapes, etc. Rajab et al. (1991) describe a method of detecting cracks using changes in natural frequencies. At least the lowest three bending natural frequencies need to be measured. A mathematical model of a cracked shaft has been developed using J-integral concepts. Detailed curves can be prepared from analytical results for changes in natural frequency for crack location and crack depth. Maynard et al. (2001) state that changes in lateral natural frequencies cannot be a reliable indicator because they can easily be affected by factors unrelated to cracks, such as seal ring locking, rubs, stiffness change in bearing, etc. Torsional natural frequencies, on the other hand, are not so easily affected. They can also be calculated quite accurately due to almost no damping and simpler theoretical considerations. Maynard et al. demonstrate the feasibility of using changes in torsional natural frequencies as indicators of shaft cracks. They also describe the transducer/instrumentation setup and steps to avoid common errors due to faulty instrumentation, etc.

2.4.3. Non-Traditional Methods

In this section we review papers dealing with non-traditional methods of shaft crack detection such as;

- I. Neural networks,
- II. Fuzzy logic,
- III. Borescope inspection and
- IV. Sophisticated signal processing techniques, e.g. wavelet and Wigner-Ville transforms, among others.

Papers on automated and expert systems based crack detection are also reviewed here. Two papers deal with the rather intriguing problem of estimating the re-inspection time for large turbine rotors. Rosard et al. (1994) present an on-line crack monitoring system installed in a

utility steam turbine. The system continuously measures the steam parameters at the inlet and the outlet of the high-pressure cylinder. A FE-based program then computes rotor temperatures, thermal and mechanical properties of the rotor material, and thence the operating stresses and corresponding crack growth rates for various points on the rotor. Information regarding previously detected cracks can be input to the program, which then predicts the safe operating period for any given operating conditions and also the duration before another exhaustive borescope inspection is necessary. Brose and Jirinec (1992) calculate the re-inspection time based on the crack sensitivity and growth rate observed in a test piece of identical material as the rotor. Both creep induced and fatigue induced cracks were studied. The linear elastic fracture mechanics model was used for fatigue cracks, while the creep cracks were evaluated using the C_t parameter (a far-field creep fracture parameter based on the stress power release rate) methodology. Based on the study, it was decided that creep was the predominant mechanism over fatigue for crack growth and the re-inspection time of a 30-year-old turbine rotor was proposed as six years.

Adewusi and Al-Bedoor (2002) apply neural networks for crack detection. Experimental vibration signals of rotors with and without a propagating crack are used to train multilayer, feedforward neural networks using a back-propagation algorithm. It is claimed that a two-neuron network could detect a propagating crack while a three-neuron network could detect both propagating as well as non-propagating cracks. Dirr and Schmalhorst (1988) conducted fatigue bending experiments on a stationary cracked shaft. Fatigue beach marks so formed were used to measure the crack depth and the actual shape of the cracked cross-section. These results are compared with those obtained using the DC-potential method applied to the same cracked cross-section. A FE model for the cracked region of the rotor is created using three-dimensional 20-node elements. Shaft models of different sizes and geometries can then be constructed and correlations can be made between the measured DC potential and crack

depth. Zhao and Luo (1989) discuss yet another interesting method for detecting cracks. A pair of diametrically opposed eddy-current probes is used to pick up the shaft displacements at a particular location. The signals of the two probes are then vectorially added. This removes the contribution of the shaft vibration. The sum is then converted to the frequency domain. In the case of uncracked shafts, the output after addition is zero. On the other hand, it is non-zero in the case of cracked shafts due to the extra-vibratory nature of shaft displacements. Thus, cracks can be detected by moving a pair of probes along the entire length of the rotor. Shiohata et al. (1987) patented a crack detection method based on the fact that vibration signals are essentially symmetrical when the machine is under steady operation. The shaft vibrations (in the vertical direction) at each bearing are continuously recorded and digitized. The area of the upper half (positive) for each cycle of the signal is divided by the area of the lower half (negative). Area ratios close to unity indicate the absence of cracks or a non-propagating crack. In the case of a propagating crack, the area ratios are greater than 1.06.

Imam et al. (1989) discuss the development of an automatic on-line crack detection system based on vibration histograms. The primary aim is the detection of cracks when they are less than 1% of the shaft diameter. It is stated that, for very small cracks, the changes in $2x$ magnitude and phase are more than any other component. Steady-state, start-up and run-down and temperature transition cases are continuously monitored. The rate of change of $2x$ vibration and phase is used to distinguish this from misalignment based vibrations (Muszynska, 1989). The patent by Imam et al. (1993) demonstrates the application of this method. Carlson et al. (1988) employ a similar philosophy to Imam et al. (1989), but have extended the system to identify rubs, shaft bows, misalignment and assembly problems.

Herbert (1987) describes a method for post-analysis of coast-down vibration data similar to Imam et al. (1989). He states that coast-down data are more informative than steady-state data at any single speed. He also proves mathematically that a steadily increasing trend of 2x and 3x components can be used to automatically detect cracked shafts. Zhao and Luo (1992) present a self-learning, fuzzy logic based expert system for crack identification. Diagnosis is based on the unique vibration behavior of cracked shafts. Fuzzy logic has a set of rules for deciding whether a high vibration condition is due to cracks or other reasons such as imbalance and misalignment. It also receives information from the self-learning loop every time its decisions are overruled by a human diagnostician. Thus, over a period of time, the system is fully adapted to a particular machine's behaviour and past history. Rieger and El-Shafei (1996) present an overview of the available technologies for automated fault diagnosis of critical equipment. Four commonly used technologies are compared: statistical data based condition evaluation, spectral analysis, diagnostics using parametric models and non-parametric model based (fuzzy logic, neural networks, genetic algorithms) diagnostics. It is shown how each method is better suited for a different set of malfunctions. Rieger and El-Shafei are of the opinion that a truly automatic system should distinguish between condition monitoring and fault diagnostics. A future complete system would employ a combination of some or all of the four currently used techniques.

He et al. (2001) treat crack detection in rotating shafts as an inverse problem and, based on genetic algorithms, a rotor crack detection strategy is proposed. The rotor crack detection scheme is then formulated as an optimization problem by means of the FEM and genetic algorithms are utilized to search for the solution. Sekhar (2004) uses the continuous wavelet transform (CWT) to extract sub-harmonics from the coast-down time domain vibration signal from journal locations of cracked rotors on fluid film bearings. Wavelet time–frequency analysis is a recent transformation technique developed for analysing non-stationary time

domain signals. Characteristic sub-harmonic peaks, which cannot be detected by normal fast Fourier transform (FFT) due to the non-stationary nature of the signals, can be detected by CWT. The CWT of a time-varying function $f(t)$ is defined as the sum over all time of the signal multiplied by the scaled shifted versions of the wavelet function (ψ). Mathematically it is expressed as follows: The Morlet mother wave has been chosen for the present application. The coast-down CWT of a rotor stopped from the supercritical range can clearly show sub-harmonics and can give away the presence of a crack. Zuo et al. (2002) also employ CWT for crack detection. They use the hinge model of a crack and numerically simulate the behaviour of a cracked shaft. A dynamic algorithm is developed to detect cracked shafts from the sampled vibration data. According to Zuo et al., the correct sampling frequency is critical for accurate transforms. They suggest a sampling frequency range of 32–64 times the shaft running speed. The CWT of the uncracked or accurately modeled mathematical rotor is continuously compared with the CWT of the running rotor. The paper outlines the several differences between the two, which can be applied for crack detection. Feldman and Seibold (1998) use the Hilbert transform (HT) to detect non-linearities from the measured vibration of a rotor. The HT converts the signal into a slowly-varying envelope type signal and a phase angle. Basic vibration data, such as stiffness, system damping, etc., can be deduced from this. Identification algorithms, based on the extended Kalman filter (EKF) and the instrumental variables method can then be applied to the transformed data to detect cracks. The EKF is a time domain identification algorithm and Seibold et al. (1996) and Seibold and Weinert (1996) show that the depth of the crack can be calculated correctly, even if the measurement information is incomplete. The localization is performed by designing a bank of EKFs, in which each filter is tuned to a different damage hypothesis, i.e. in this case the specific crack location. By calculating the probabilities of the different hypotheses, the crack can be localized and its depth can be determined. The procedure is applied to a simulated rotor and

also to a rotor test rig. The dynamic equation of transient response in a cracked rotor is modelled, and is based on the simple hinge crack model. The numerical simulation solutions of the uncracked rotor and the cracked rotor are obtained from the model.

Zou et al. (2003) use the Wigner-Ville transformation, which is yet another tool to analyse non-stationary, non-linear systems. They model a cracked Jeffcott rotor and numerically obtain the response. The time–frequency features of the cracked rotor and the uncracked rotor are compared, and a new algorithm is proposed using the Wigner-Ville distribution to identify the cracked rotor. Upon transformation from the time domain to the time and frequency domain, the sub-harmonic content is clearly visible. By simulation research, the sensitivity of the Wigner-Ville distribution to the stiffness variation is investigated, and the influence of the unbalance and the inhabiting angle on the time–frequency feature is discussed.



CHAPTER 3 MATERIALS AND METHODS

3.1 Torsional Vibration Experiment

Torsional vibration is an oscillatory angular motion causing twisting in the shaft of a system. The processes leading to the conduct of the torsional vibration experiment are elaborated in the next sections.

3.1.1 Shaft Material Selection

The material used for the cracked shaft specimens in this work was AISI 1020 mild steel. AISI 1020 mild steel, cold drawn, was chosen for the experiment because it is referred to by the American Iron and Steel Institute (AISI) as a standard shaft material.

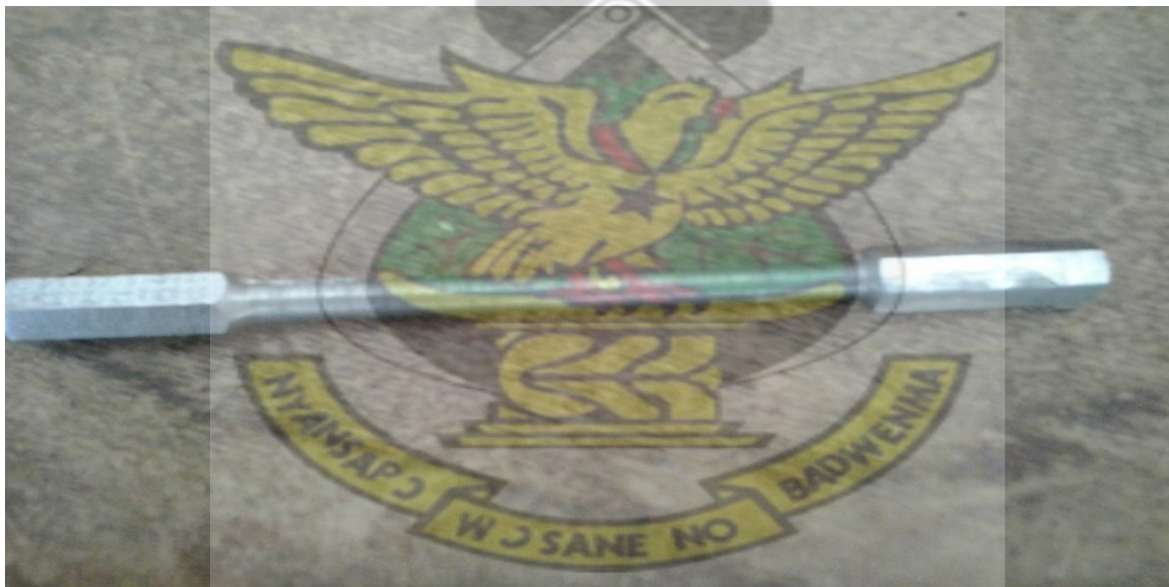


Figure 3.1: AISI 1020 mild steel shaft specimen

The material properties of AISI 1020 mild steel are shown in Tables 3.1, 3.2 and 3.3

Table 3.1: AISI 1020 mild steel, cold drawn

Category	Steel
Class	Carbon steel
Type	Standard
Designations	France: AFNOR CC 20 Germany: DIN 1.0402 Italy: UNI C 20 Sweden: SS 1450 United Kingdom: B.S. 040 A 20 , B.S. 070 M 20 United States: AMS 5032 , AMS 5032B , AMS 5045 , AMS 5045C , ASTM A108 , ASTM A29 , ASTM A510 , ASTM A519 , ASTM A544 , ASTM A575 , ASTM A576 , ASTM A659 , MIL SPEC MIL-S-11310 (CS1020) , SAE J403 , SAE J412 , SAE J414 , UNS G10200

Source: (eFunda, Inc. 2014)

Table 3.2: Material composition of AISI 1020 mild steel, cold drawn

Element	Carbon (C)	Iron (Fe)	Manganese (Mn)	Phosphorous (P)	Sulphur (S)
% Weight	0.18-0.23	99.08-99.53	0.30-0.60	0.04(max)	0.05(max)

Source: (eFunda, Inc. 2014)

Table 3.3: Mechanical Properties of AISI 1020 mild steel, cold drawn

Physical Properties	Value
Density ($\times 1000 \text{ kg/m}^3$)	7.70-8.03
Poisson's Ratio	0.27-0.30
Bulk Modulus (Gpa)	140
Tensile Strength (Mpa)	394.7
Yield Strength (Mpa)	294.8
Elongation (%)	36.5
Reduction in area (%)	66.0

Source: (eFunda, Inc 2014)

3.1.2 Shaft specimen creation

The specimen used as earlier indicated was obtained from a mild steel material by machining. In all, ten specimens were made.

3.1.3 Dimensions of the shaft specimen

The dimensions for the specimen is indicated in Figure 3.2

- The total length of the specimen was 143 mm.
- The test section was cylindrical in nature; 76 mm long and 8 mm in diameter.
- Both ends of the specimen were hexagonal in shape with a dimension of 11.3 mm across flat.

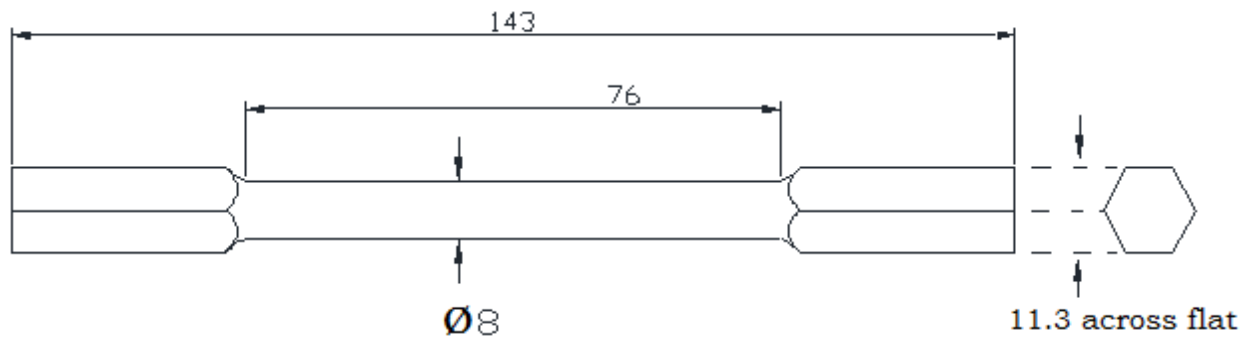


Figure 3. 2: Shaft specimen dimension (All dimensions in mm)

3.1.4 Shaft crack shape

As discussed earlier, a transverse crack caused by material fatigue is a very common defect in rotating equipment that operates for extended periods under heavy load. This type of crack remains the most important type of crack as the machine safety is significantly influenced by its occurrence.

The crack shape used was based on two criteria;

- I. The ease with which the crack can be mimicked in the lab
- II. Our knowledge on fracture mechanics on crack initiation.

Based on the above criteria, a V-notch shape was chosen, since crack propagation at its tip is a common occurrence, as such its early detection is crucial.

The crack type used was an open crack (notch) since it is easy to mimic in the lab. The choice of the shape is based on knowledge of fracture mechanics where fatigue transverse cracks are known to propagate in a semi-elliptical form. Figure 3.3 shows a sketch of the notch.

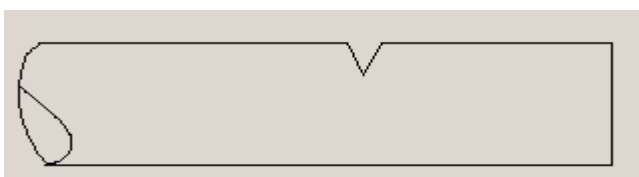


Figure 3.3: V-notch crack.

3.1.5 Generation of the crack

Usually cracks can be initiated at the point which has the maximum local stress and the minimum local strength. The local stress pattern is determined by the shape of the shaft, as well as the type and magnitude of the loading.

In this work, the test section of the shaft specimen is cylindrical in shape. The specimen was clamped with a vice and the swivelling action of a tool bit placed in the tool post was used to create the v-notch crack on the shaft.



Figure 3.4: Shaft specimen with a v-notch crack

3.1.6 Shaft crack position and depth

This work involved the creation of three v-notch cracks of depths: 1.0 mm, 2.0 mm & 3.0 mm at three different positions (25 mm, 38 mm & 51 mm) from one end of the shaft specimen. For the first specimen, a 1 mm crack depth at a position of 25 mm from the left end was made on the shaft specimen. A 1 mm crack depth was made at the centre (38 mm from left end) and at a distance of 51 mm from the left end on the second and third shafts respectively.

A crack depth of 2 mm was made at a position of 25 mm, 38 mm and 51 mm on the fourth, fifth and sixth shafts respectively. The procedure was repeated for a crack depth of 3 mm at

positions 25 mm, 38 mm and 51 mm from left end of shafts seven, eight and nine respectively. The tenth shaft was left intact with no crack.

3.1.7 Instrumentation for Torsional experiment

The instruments used in the experiment are indicated below;

1. Milling machine: the hexagonal end of the shaft specimens (ten in number) were obtained from a cylindrical mild steel rod (12mm diameter and 1.5m long) by carrying out a milling operation on a milling machine.
2. Lathe machine: the cylindrical section of the shaft specimen was obtained by carrying out a turning operation on the centre lathe machine.
3. Shaping machine: the creation of the v-notch crack on the shaft was done by means of a tool bit placed in the tool post of the shaping machine.
4. Torsion testing machine: the experimental work was done using *Tecquipment SMI MKII*-torsion testing machine.

3.1.8 Torsional Vibration Experimental Work

The experimental investigation was carried out on a *Tecquipment SMI MKII*-torsion testing machine shown in Figure 3.5. In order to study the response of materials under a torsional force, the torsion test was performed by mounting the specimen onto a torsion testing machine and then applying the twisting moment.



Figure 3.5: Tecquipment SMI MKII-torsion testing machine

The hexagonal ends of the cylindrical shaft specimen are tightened to hexagonal sockets in which one is fitted to a torque shaft and another is fitted to an input shaft. The twisting moment is applied by turning the input handwheel to produce torque.

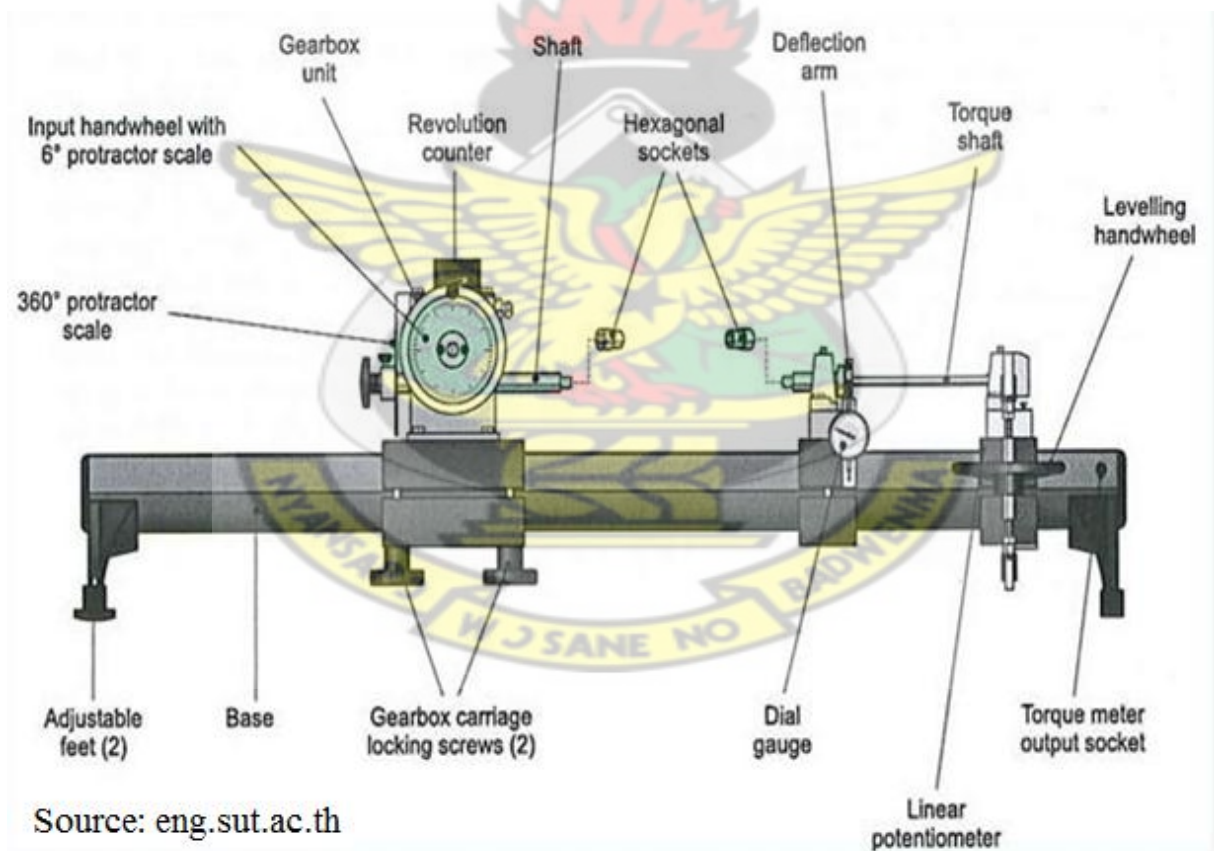


Figure 3.6: Schematic diagram showing details of torsion testing machine

When the twisting moment is applied, the torque is reacted by a torque shaft, which moves in relation to the deflection arm. The movement of the deflection arm is measured by a linear potentiometer, which is connected to a calibrated TQ digital torque meter shown in Figure 3.6 to give readout of the torque in a unit of Nm.



Figure 3.7: Digital torque meter

The shaft with no crack was first placed in the hexagonal socket fitted to a torque shaft and the other end fitted to an input shaft. The twisting moment is applied by turning the input handwheel to record the angle of twist and the corresponding torque recorded by means of a digital torque meter. The procedure was repeated for the nine shaft specimen with varying crack depths and positions. The angle of twist was recorded and the corresponding torque also recorded.

3.2 Transverse Vibration Experiment

Transverse vibration refers to periodic disturbances for which the particle oscillations of the medium are perpendicular to the direction of propagation. The frequency of transverse vibrations of a beam with bodies attached is identical to the critical (whirling) speed of a shaft of the same stiffness as the beam, carrying discs of masses which correspond to those of the bodies on the beam. One has to think in terms of small size rotors, otherwise gyroscopic

effects are involved. The processes used for the transverse vibration experiment are outlined in the next sections.

3.2.1 Shaft Material selection and Creation

The material used for generating the cracked shaft specimen in the transverse vibration experiment was AISI 1020 mild steel. The desired shape (which is explained in detail in the next section) was obtained by a machining operation on a milling and lathe machine.

3.2.2 Dimensions of the shaft specimen

The dimensions used for the experiment is shown in Figure 3.8.

1. The total length of the shaft specimen is 838 mm
2. The test section is cylindrical in nature; 736 mm long and 15 mm in diameter.
3. Both ends of the specimen are rectangular in shape, with a width of 11 mm.
4. One end of the rectangular section is 36 mm long and the other end 66 mm long.

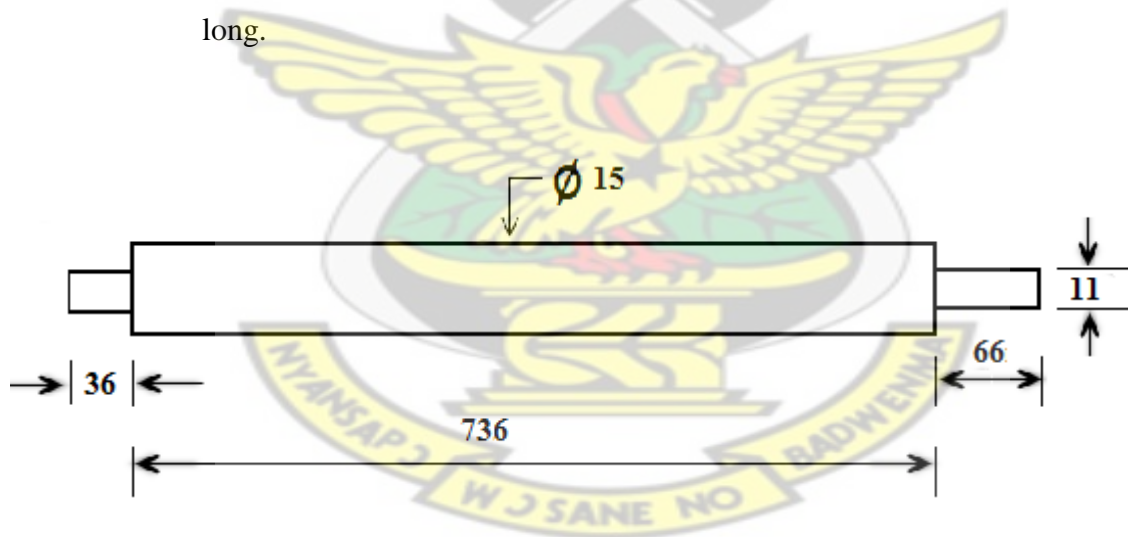


Figure 3.8: Dimensions for the transverse vibration shaft specimen (All dimensions are in mm)

The dimensions in Figure 3.8 were used in order to fit into the experimental setup (*Tecquipment TM16 Universal Vibration Apparatus*).

3.2.3 Generation of crack

The specimen was clamped with a vice and the cut made with a hacksaw. The hacksaw was used this time around to prevent the removal of large quantities of material.



Figure 3. 9: Shaft surface crack

3.2.4 Shaft crack position and depth

The shaft used for the transverse vibration experiment had saw-cut crack depths (2.5 mm, 5.0 mm and 7.5mm) at three different positions (200 mm, 368 mm & 536 mm) on the shaft specimen. For the first specimen, a 2.5 mm crack depth at a position of 200 mm is made on the shaft specimen. A 2.5 mm crack depth is made at the centre (368 mm) and at a distance of 536 mm on the second and third shafts respectively.

A crack depth of 5.0 mm is made at a position of 200 mm, 368 mm and 536 mm on the fourth, fifth and sixth shafts respectively. A crack of 7.5 mm depth is made at a position of 200 mm, 368 mm and 536 mm on seventh, eighth and ninth shafts. The tenth shaft is left intact with no crack.

3.2.5 Instrumentation for Transverse experiment

1. **Milling machine:** the rectangular section of the shaft specimen was obtained from a cylindrical mild steel rod by carrying out a milling operation on a milling machine.

2. **Lathe machine:** the cylindrical part of the specimen was obtained by a turning operation on a lathe machine.
3. **Hacksaw:** the creation of the saw-crack on the shaft was done by means of a hacksaw.
4. **Transverse testing machine:** the experimental work was done using Tecquipment TM16 Universal Vibration Apparatus.

3.2.6 Transverse Vibration Experimental Work

The apparatus for this experiment is indicated in Figure 3.10. The shaft specimen is supported at each end by trunnion blocks. The right-hand support pivots in two ball bearings in a housing located on the inside face of the vertical frame member. The left-hand support consists of two roller bearings, which are free to move in a guide block located on the inside face. A small motor is bolted to the centre of the shaft specimen. The motor is connected via leads to a precision speed control unit, which applies a wide range of exciting frequencies to the shaft specimen.



Figure 3. 10: Transverse vibration experimental setup.

The experimental procedure involves first placing the shaft specimen without a crack in the support bearing of the trunnion blocks. The specimen is held firmly in place by tightening the screw on top of each trunnion block. The motor was connected to the speed control unit via leads and bolted to the middle of the shaft specimen. When the power from the mains is switched on, clockwise rotation of the control knob on the speed control unit increases the speed of the motor. As the speed increases as indicated by the speed meter on the control unit, the shaft begins to vibrate transversely. Over a discrete band of frequencies, increasingly larger amplitudes of vibration are produced which reach a peak at a frequency corresponding to the frequency of free natural transverse vibration of the system (shaft specimen). In order to determine accurately the exact value on the speed meter, it was expedient to take the shaft specimen through the range of excessive amplitudes several times, noting the limits from the range. From these, the frequency at which the amplitude and resultant noise appears greatest was located. The probe of a digital vibration meter shown in Figure 3.11 was attached to the shaft to record the corresponding acceleration.



Figure 3. 11: Digital vibration meter.

The procedure is repeated for the shaft with a 2.5 mm crack depth at a position of 200 mm from the left. The frequency of excitation corresponding to the frequency of free natural acceleration of vibration is then measured with the digital torque meter. The experimental procedure is repeated for the other eight shafts with different crack depths and positions. The results are recorded in Table 4.3.

4.3 Theoretical Approach

3.3.1 Analytical Approach (Dunkerley's method)

The natural frequency of transverse vibration for a shaft carrying one or more point loads and uniformly distributed load is obtained from Dunkerley's empirical formula. According to this

$$\frac{1}{f^2} = \frac{1}{f_1^2} + \frac{1}{f_2^2} + \frac{1}{f_3^2} + \dots + \frac{1}{f_s^2}$$

Where f = the natural frequency of transverse vibration of the shaft carrying point loads and uniformly distributed load.

$f_1, f_2, f_3, etc.$ = Natural frequency of transverse vibration of each point load acting alone.

f_s = Natural frequency of transverse vibration of the uniformly distributed load (or due to the mass of the shaft)

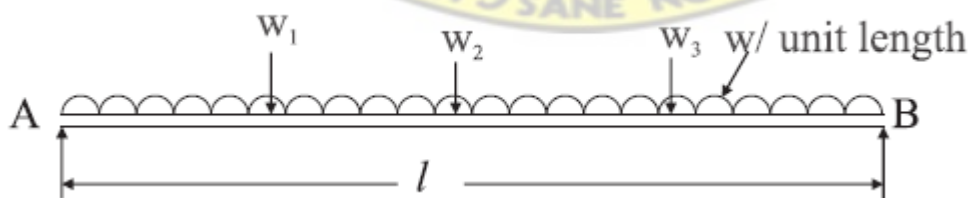


Figure 3. 12 Shaft with point and uniformly distributed load

Let $\delta_1, \delta_2, \delta_3, etc$ = Static deflection due to the loads W_1, W_2, W_3, etc where considered separately.

δ_s =static deflection of the uniformly distributed load or due to the mass of the shaft.

Therefore according to Dunkerley's empirical formula, the natural frequency of the whole system is;

$$f = \frac{0.4985}{\sqrt{\delta_1 + \delta_2 + \delta_3 + \dots + \frac{\delta_s}{1.27}}} \text{ Hz}$$

The values of $\delta_1, \delta_2, \delta_3$ etc for a simply supported shaft may be obtained from the relation

$$\delta = \frac{W a^2 b^2}{3EI l}$$

Where

δ = static deflection due to load W,

a and b =distances of the loads from the ends,

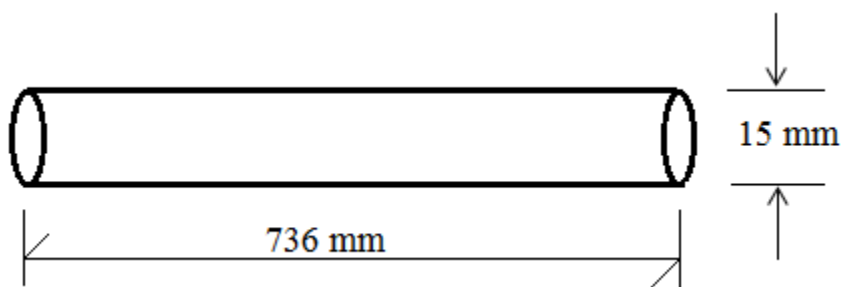
E =Young's modulus for the material of the shaft,

I =Second moment of area of the shaft, and

l =Total shaft length.

From the above theory, the natural frequency was computed as follow;

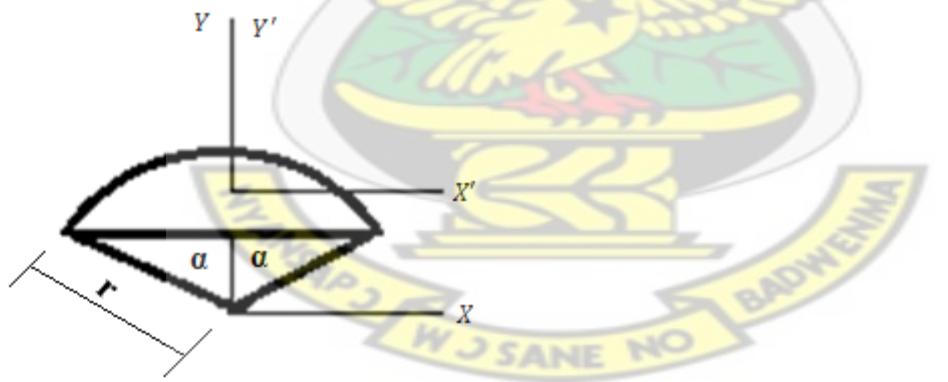
Shaft dimension (test section)



The test section had the following data;

1. Mass (m) = 1.03 kg
2. Density (ρ) = $7890 \frac{kg}{m^3}$
3. Volume (v) = $\pi r^2 l m^3$
4. Radius (r) = 7.5 mm
5. Length (l) = 736 mm
6. Elastic modulus (E) = 210 Gpa
7. Second moment of Area, $I = \frac{\pi d^4}{64} (m^4)$
8. Diameter (d) = 15 mm
9. Point load position (a) = 368 mm

With the introduction of the crack, there is a variation in some of the parameters and they are computed as follow;



- I. $\theta = 2 \cos^{-1} \left(\frac{r-d'}{r} \right)$, where $\theta = 2\alpha$
- II. Crack depth (d') = 0, 2.5 mm, 5.0 mm, 7.5 mm
- III. Area of crack section (taken-off), $A_c = \frac{r^2}{2} \left(\frac{\theta\pi}{180^\circ} - \sin \theta \right)$
- IV. Volume of crack section (taken-off), $V_c = A_c w$
- V. Where, $w = \text{width of crack} = 1 \text{ mm}$

- VI. Mass of cracked part (taken-off), $m_c = \rho V_c$
- VII. Mass of shaft with crack part taken-off, $m_s = m - m_c$
- VIII. Static deflection due to point load, $\delta_m = \frac{Wa^2b^2}{3EI} = \frac{mga^2b^2}{3EI}$
- IX. Where, $a=368$ mm and $b=368$ mm
- X. Static deflection due to shaft mass $\delta_s = \frac{5}{384} \times \frac{wl^4}{EI} = \frac{5}{384} \times \frac{m_s \times g \times l^4}{EI}$
- XI. Second moment of cracked section $I'_x = \frac{1}{4}r^4(\alpha + 2(\sin \alpha)^3 \cos \alpha - \sin \alpha \cos \alpha)$

From Dunkerley's empirical formula, the frequency of transverse vibration

$$f = \frac{0.4985}{\sqrt{\delta_m + \frac{\delta_s}{1.27}}} \text{ (Hz)}$$

And the critical speed (N_c) in rpm is calculated as;

$$N_c = 60f \text{ (rpm)}$$

In order to account for the position of the crack, the shaft was compartmentalised into three sections as indicated in Figure 3.13, with;

1. Section 1 representing shaft section to the left of the crack.
2. Section 2 representing the cracked section.
3. Section 3 representing shaft section to the right of the crack.

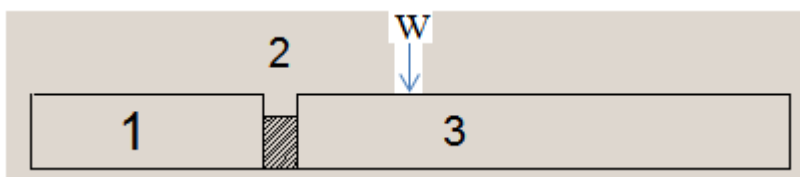


Figure 3.13 Division of cracks into sections based on the position of crack

The frequency was then calculated as;

$$f = \frac{0.4985}{\sqrt{\delta_m + \frac{\delta_{1s} + \delta_{2s} + \delta_{3s}}{1.27}}} \text{ (Hz)}$$

Where;

1. δ_{1s} = deflection caused by section 1
2. δ_{2s} = deflection caused by section 2
3. δ_{3s} = deflection caused by section 3
4. δ_m = deflection due to point load W

The above procedure was simulated using Matlab coding as indicated in appendix B.

4.3.2 Numerical method

In this method, an iterative method using finite element was applied by using Solidworks (ver. 2014). The three dimensional model shown in Figure 3.13 of the shaft was modelled using the Solidworks software.



Figure 3. 14 3-D model of the shaft

The frequency analysis for the 3-D model was analysed and meshed. Figure 3.15 shows the meshed shaft. The appropriate mesh density (fine) was chosen and the program runs.

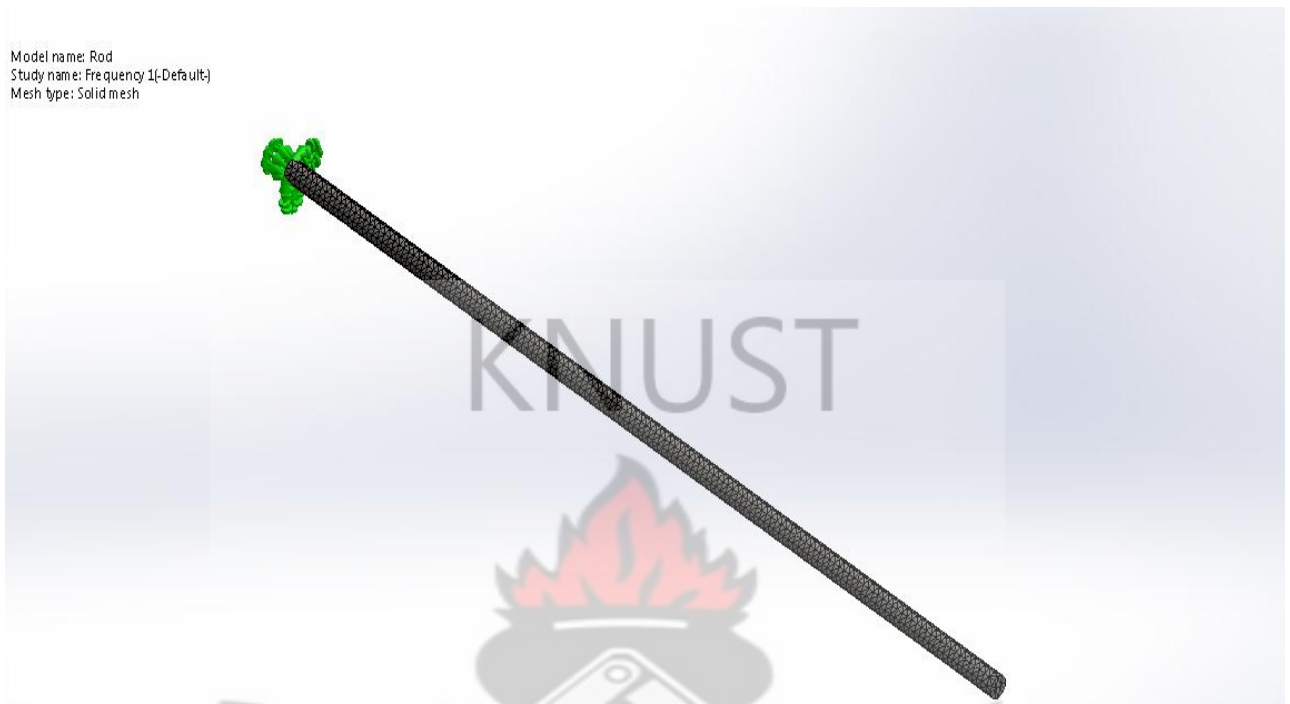


Figure 3. 15 Meshed shaft

From figure 3.15, it might appear that the shaft was modelled as a cantilever beam but that was not the case. A view indicating roller support at the other end is indicated in Figure 3.16.



Figure 3.16 View indicating support (roller) at the shaft end

The support at the end is a roller that permitted motion in the horizontal plane but restricted motion in the vertical plane. This was done to imitate the trunnion block support used in the experiment.

CHAPTER 4 Results and Discussion

4.1 Torsional Vibration Results and Discussions

4.1.1 Results

The results for the torsional vibration experiment are indicated in Tables 4.1a and 4.1b. The angle of twist in degrees and the corresponding torque in Newton-metre for various crack positions and depths is presented.

Table 4.1a: Angle of twist and corresponding Torque for different crack depths and positions.

Angle of twist (°)	Torque(Nm) for Shaft with no crack	Torque(Nm) for Shaft with 1.0 mm crack-depth at a length of 25 mm	Torque(Nm) for Shaft with 1.0 mm crack-depth at centre (38 mm)	Torque(Nm) for Shaft with 1.0 mm crack-depth at a length of 51 mm	Torque(Nm) for Shaft with 2 .0 mm crack-depth at a length of 25 mm
0	0	0	0	0	0
5	12.2	9.6	0.5	8.5	0.4
10	25.6	23.3	3.4	19.6	8.9
15	28.2	27.6	10	27.5	21.6
20	29.2	28.2	20.3	32.5	27.1
25	30.1	29	28.3	33.5	28.2
30	30.6	29.6	29.7	34.7	29.3
35	31.5	30	30.1	35	29.7
40	31.8	30.3	30.5	35.4	30.5
45	32	31.3	31	36.2	30.9

Table 4.1b: Angle of twist and corresponding Torque for different crack depths and positions.

Angle of twist (°)	Torque(Nm) for Shaft with 2.0 mm crack-depth at centre (38 mm)	Torque(Nm) for Shaft with 2.0 mm crack-depth at a length of 51 mm	Torque(Nm) for Shaft with 3.0 mm crack-depth at a length of 25 mm	Torque(Nm) for Shaft with 3.0 mm crack-depth at centre (38 mm)	Torque(Nm) for Shaft with 3.0 mm crack-depth at a length of 51 mm
0	0	0	0	0	0
5	0.6	9.2	1.2	0.6	8.5
10	10.3	18.6	9.8	10.1	19
15	23	25.7	22.7	21.5	30.3
20	25.7	29.2	32.1	30.1	34.6
25	26.7	30	35.7	32.9	35.2
30	27.2	30.9	37.6	34.4	35.8
35	27.8	32.3	37.8	35.2	35.9
40	28.6	32.3	37.8	35.4	36
45	29.2	32.7	37.4	35.6	36.4

From the above table, a graph of torque (Nm) against angle of twist(°) is plotted in order to compare the torsional rigidity of the intact shaft and a defective (cracked) one. Also for the same crack depth, at different positions, a comparison is made between their torsional rigidity. The graphs are shown from Figure 4.1 through to Figure 4.12) .

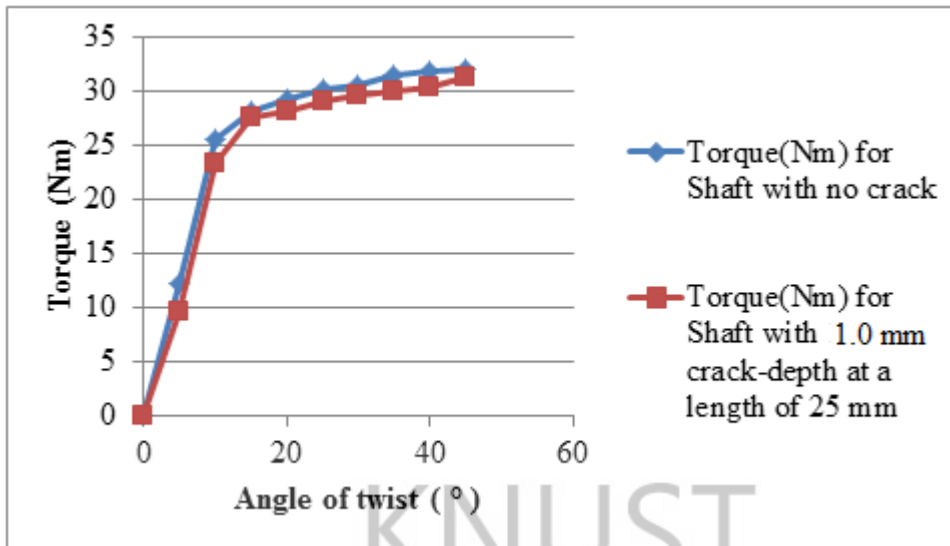


Figure 4.1: Comparison between an intact shaft and a shaft with 1 mm depth at a distance of 25 mm

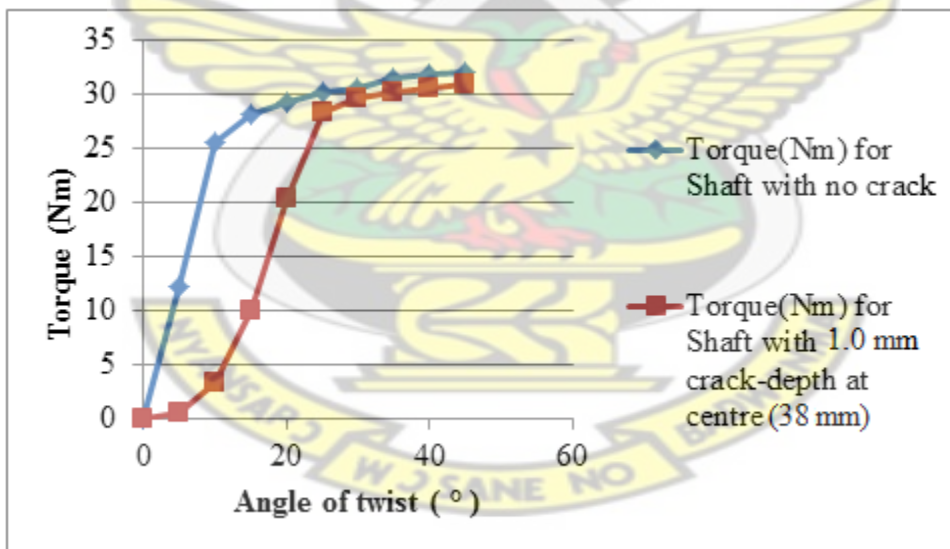


Figure 4.2: Comparison between an intact shaft and a shaft with 1 mm depth at a distance of 38 mm

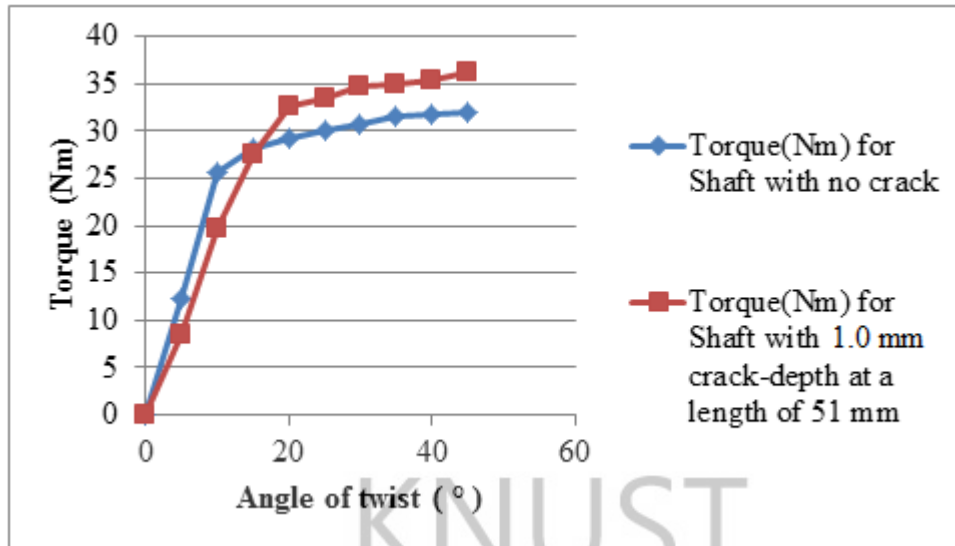


Figure 4.3: Comparison between an intact shaft and a shaft with 1 mm depth at a distance of 51 mm

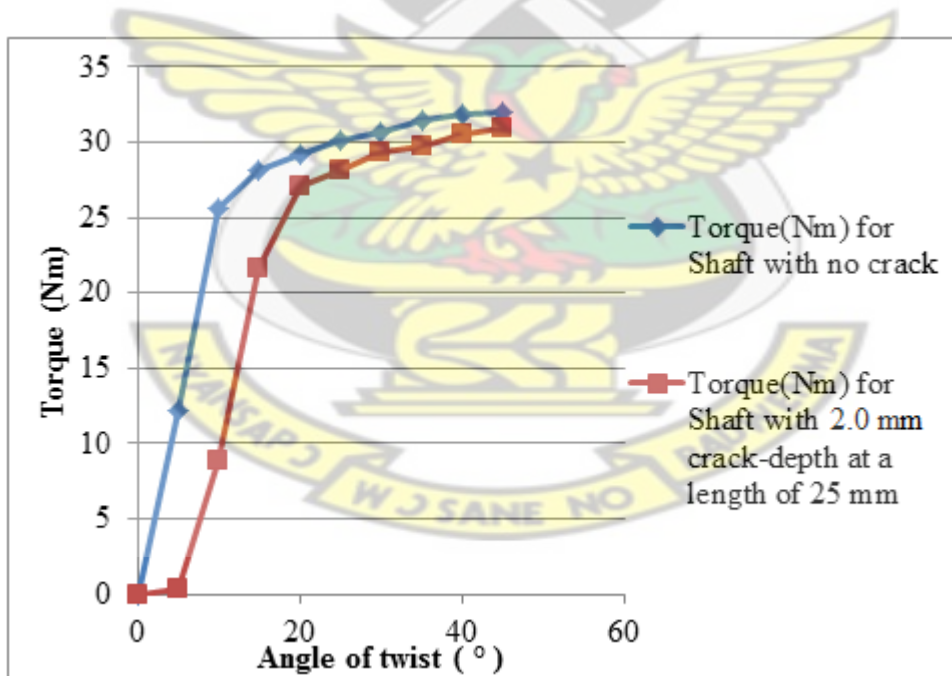


Figure 4.4: Comparison between an intact shaft and a shaft with 2 mm depth at a distance of 25 mm

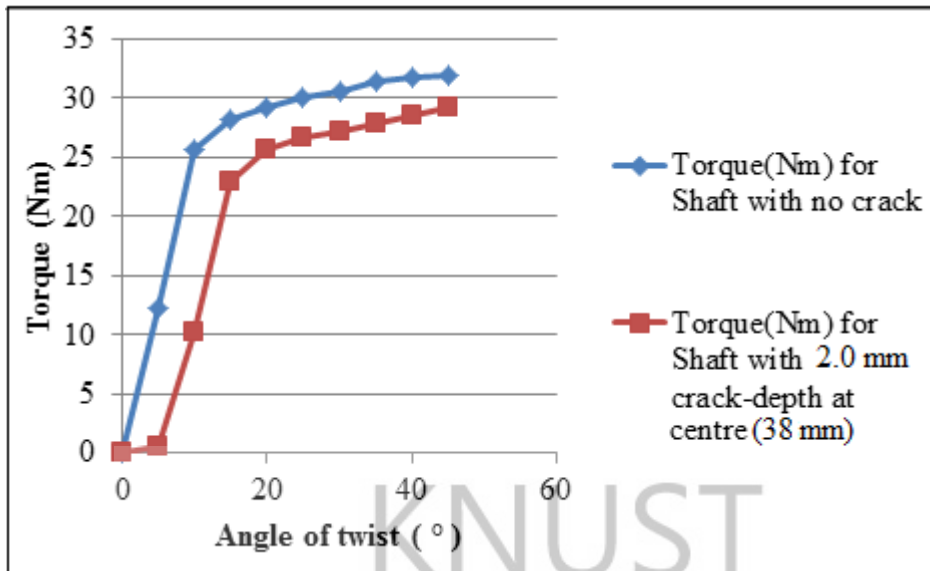


Figure 4.5: Comparison between an intact shaft and a shaft with 2 mm depth at a distance of 38 mm

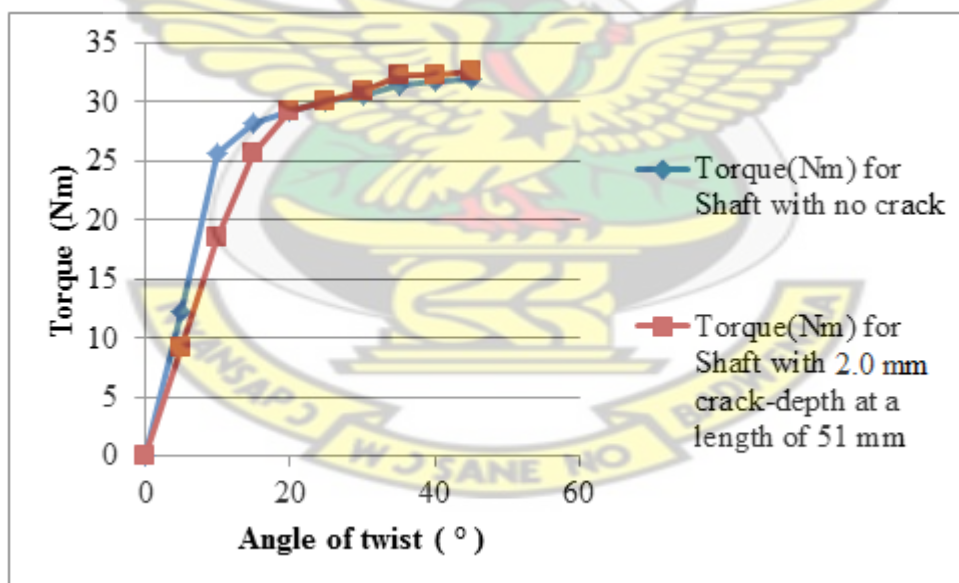


Figure 4.6: Comparison between an intact shaft and a shaft with 2 mm depth at a distance of 51 mm

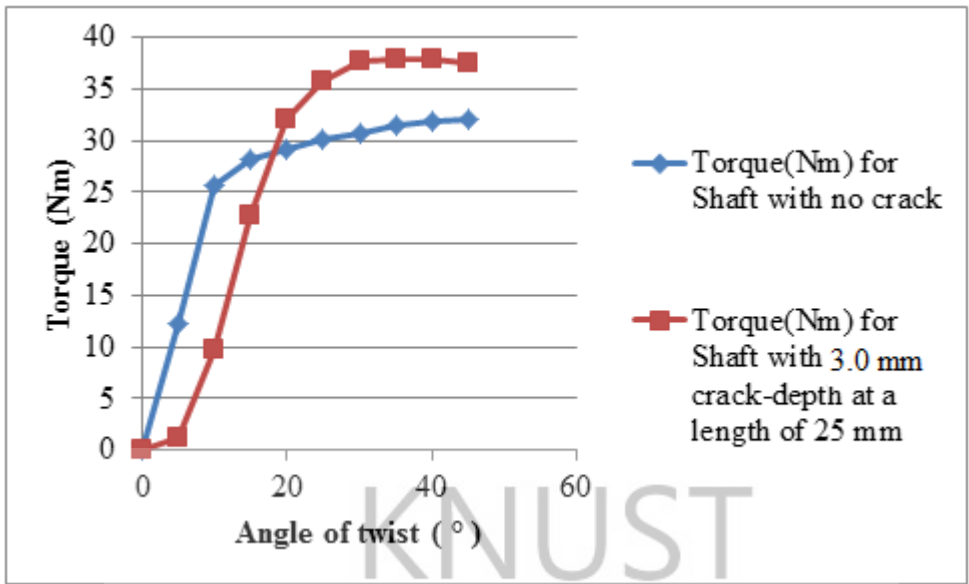


Figure 4.7: Comparison between an intact shaft and a shaft with 3 mm depth at a distance of 25 mm

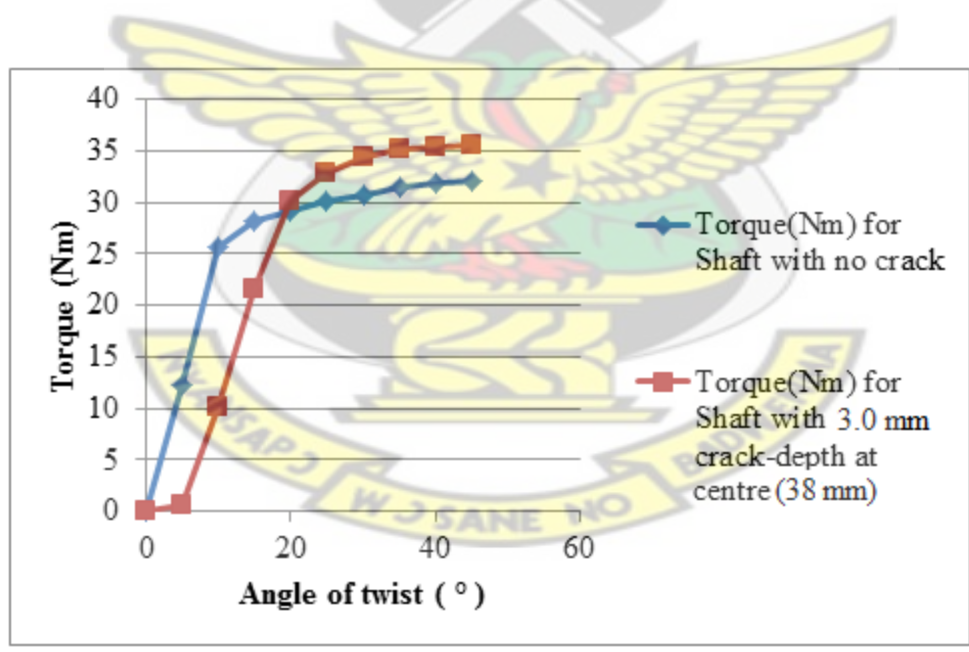


Figure 4.8: Comparison between an intact shaft and a shaft with 3 mm depth at a distance of 38 mm

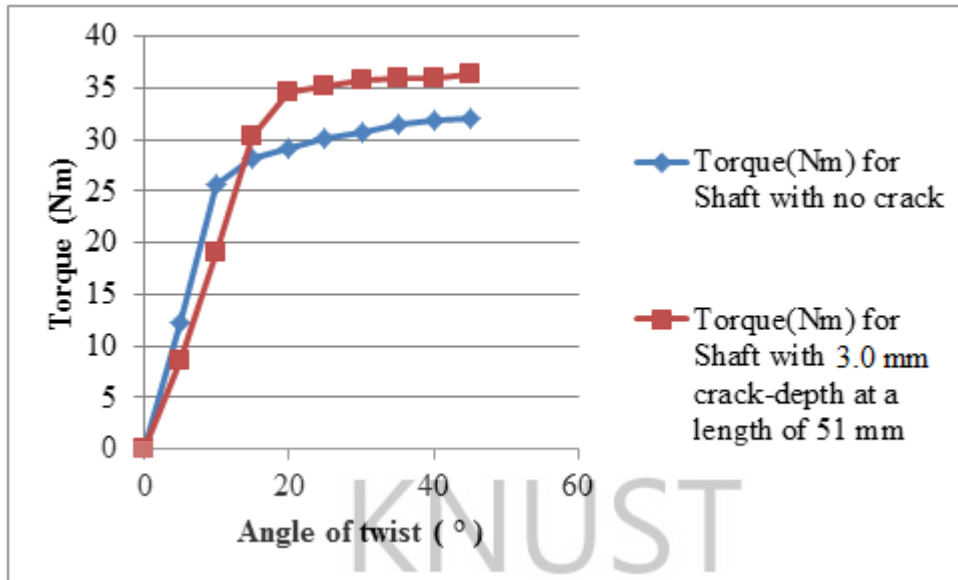


Figure 4.9: Comparison between an intact shaft and a shaft with 3 mm depth at a distance of 51 mm

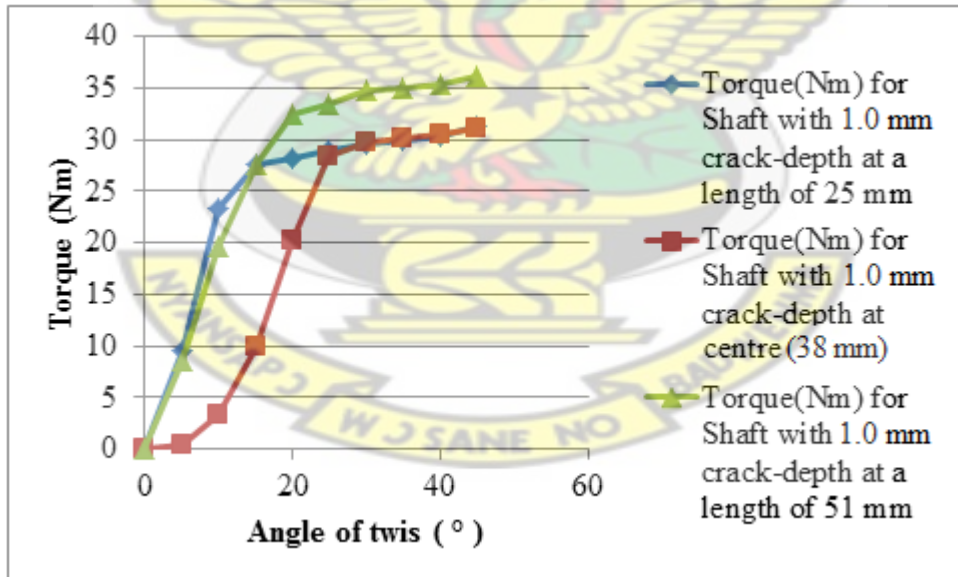


Figure 4.10: Comparison between three shafts with the same crack depth (1 mm) at different positions (25mm, 38mm & 51mm)

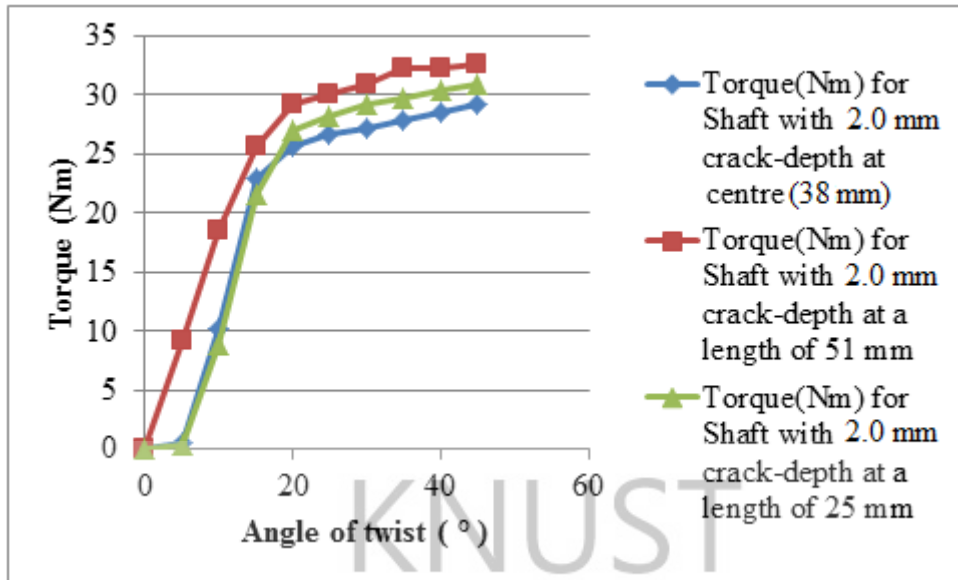


Figure 4.11: Comparison between three shafts with the same crack depth (2 mm) at different positions (25mm, 38mm & 51mm)

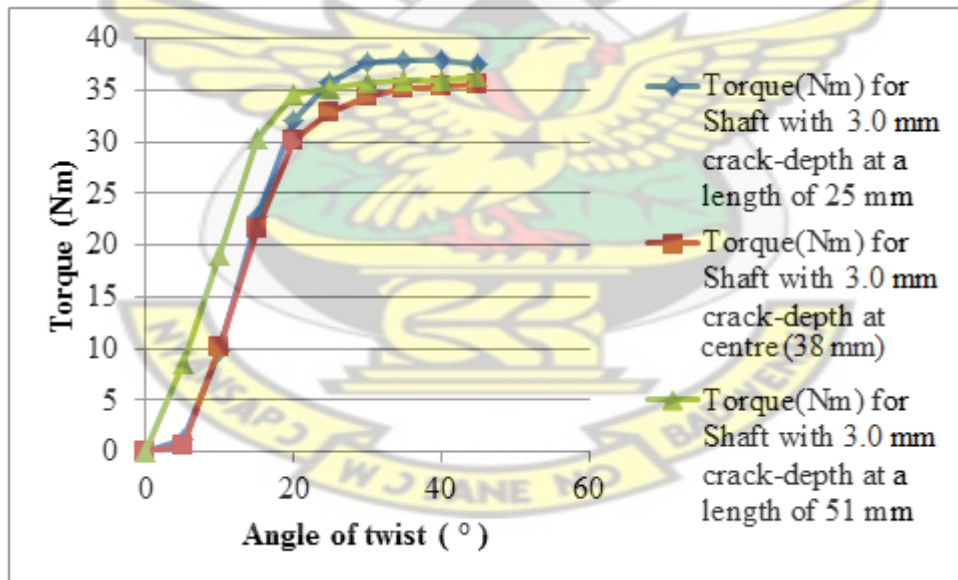


Figure 4.12: Comparison between three shafts with the same crack depth (3 mm) at different positions (25mm, 38mm & 51mm).

4.1.2 Discussions

From the data, a graph of torque (Nm) against angle of twist ($^{\circ}$) was plotted. It was observed that the defective (cracked) shafts had a lower torsional stiffness as compared to the intact shaft. The deeper the crack, the higher the reduction in torsional stiffness. For cracks with the same depth at different positions, it was observed that, their torsional stiffness varied depending on their position; with cracks at the middle (38 mm) resulting in a significant reduction in torsional stiffness as compared to those closer to the (left and right) ends of the shaft. For a crack depth of 1 mm (25% of shaft radius), there was a change in crack stiffness though marginal.



4.2 Transverse Vibration Results and Discussions

4.2.1 Results

The acceleration results for the transverse vibration experiment are indicated in appendix

Table A1. The graphs corresponding to the acceleration spectrum is indicated in Figure 4.13-

Figure 4.26.

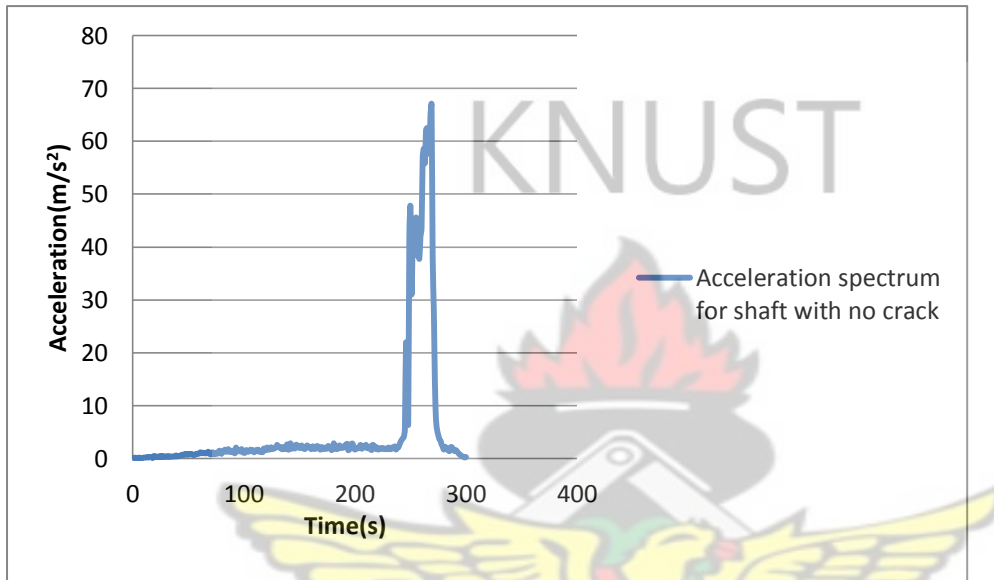


Figure 4. 13 Acceleration spectrum for shaft with no crack

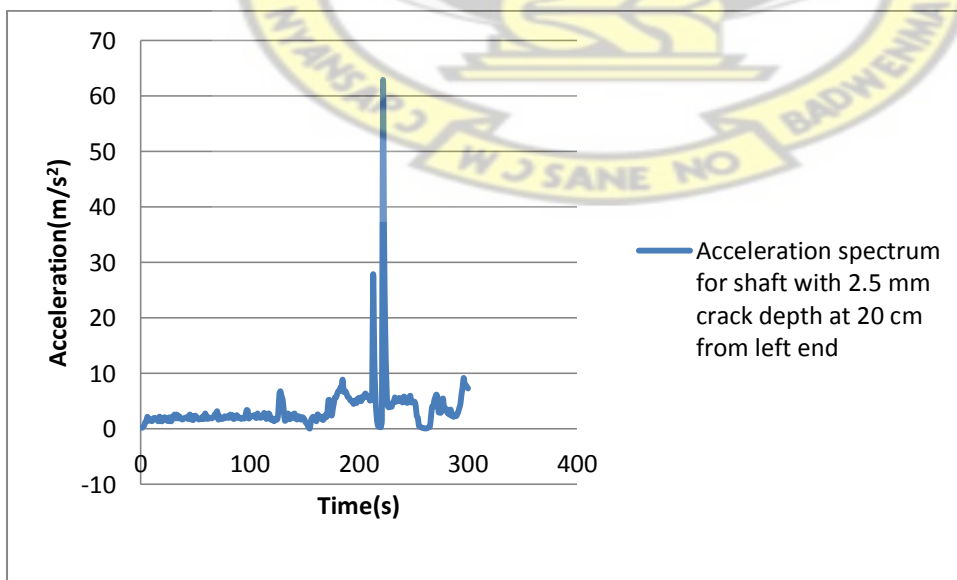


Figure 4. 14 Acceleration spectrum for shaft with 2.5 mm crack depth at 20 cm from left end

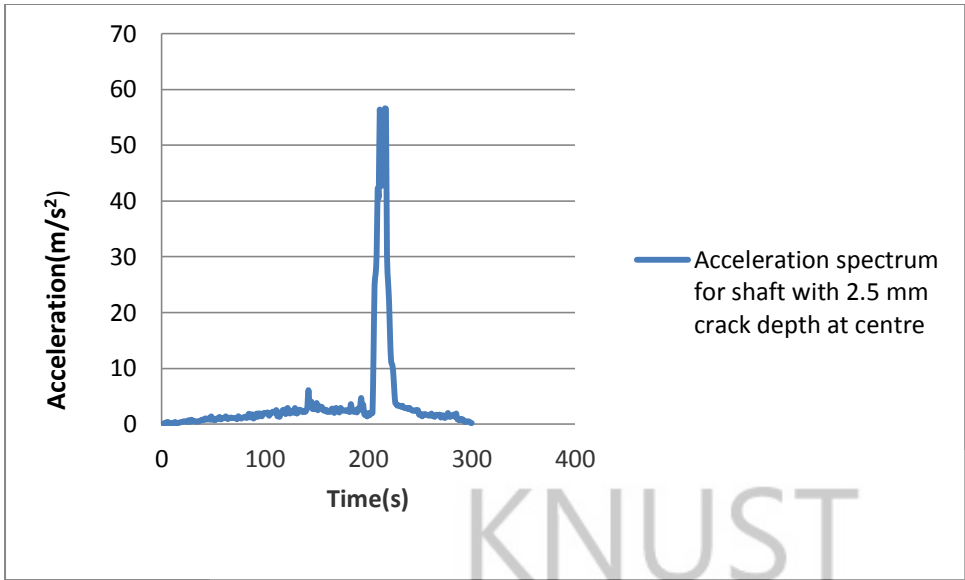


Figure 4. 15 Acceleration spectrum for shaft with 2.5 mm crack depth at centre

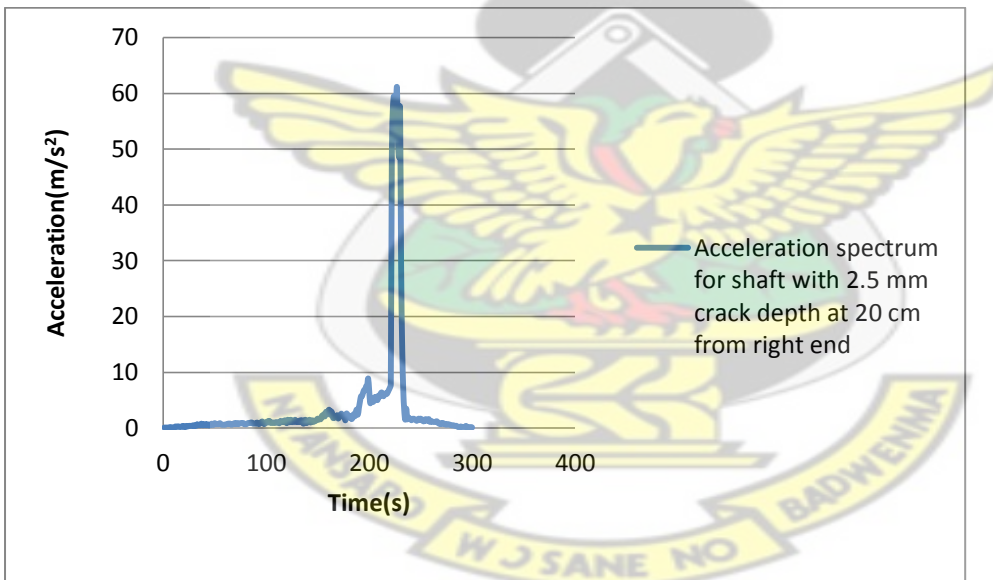


Figure 4. 16 Acceleration spectrum for shaft with 2.5 mm crack depth at 20 cm from right end

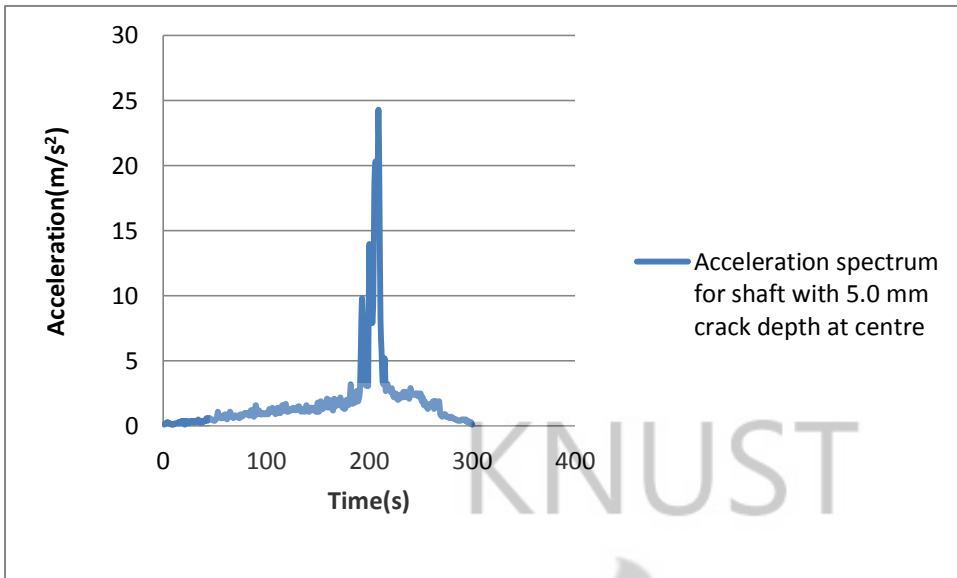


Figure 4. 17 Acceleration spectrum for shaft with 5.0 mm crack depth at centre

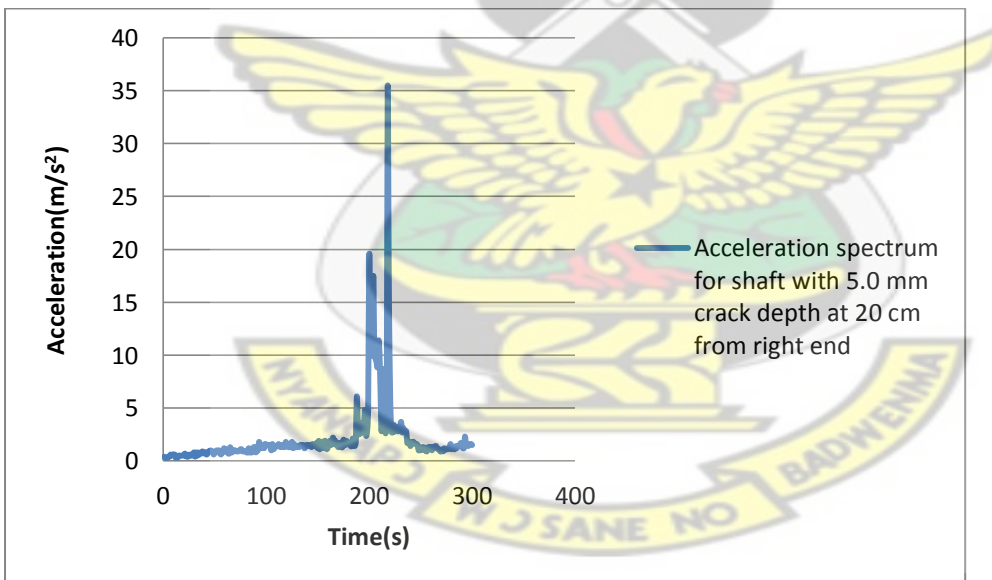


Figure 4. 18 Acceleration spectrum for shaft with 5.0 mm crack depth at 20 cm from right end

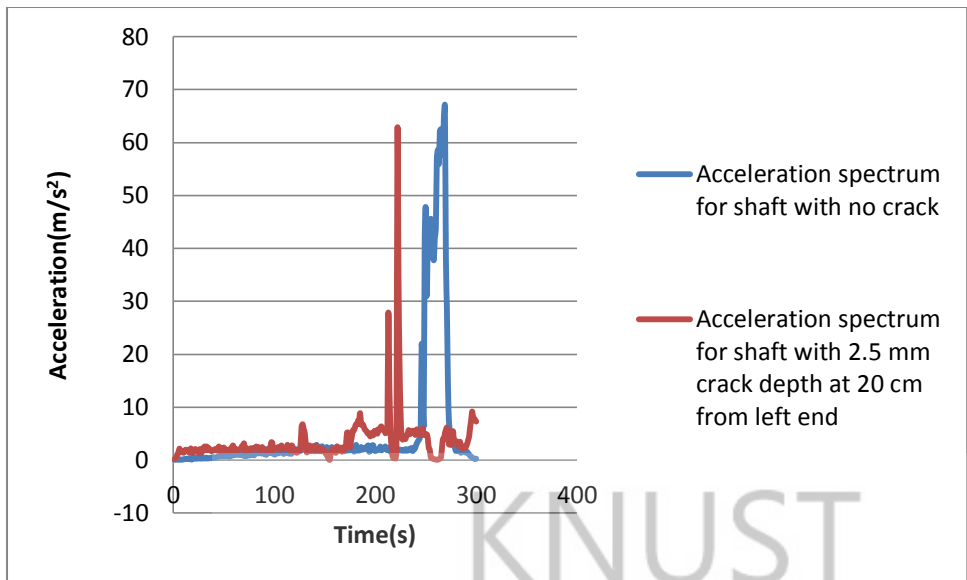


Figure 4. 19 Comparison between the acceleration spectrum of an intact shaft and a shaft with 2.5 mm crack depth at 20 cm from left end

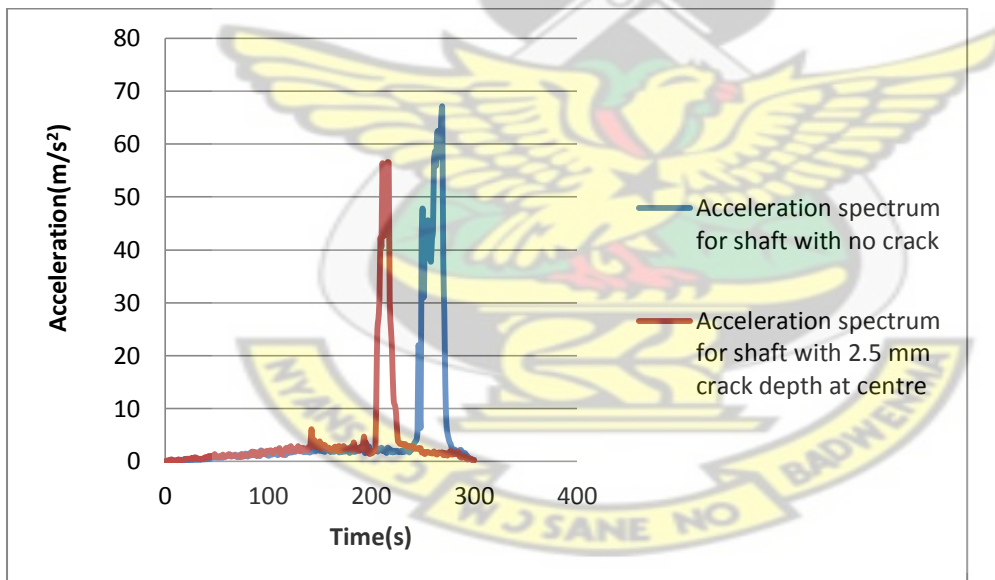


Figure 4. 20 Comparison between the acceleration spectrum of an intact shaft and a shaft with 2.5 mm crack depth at centre

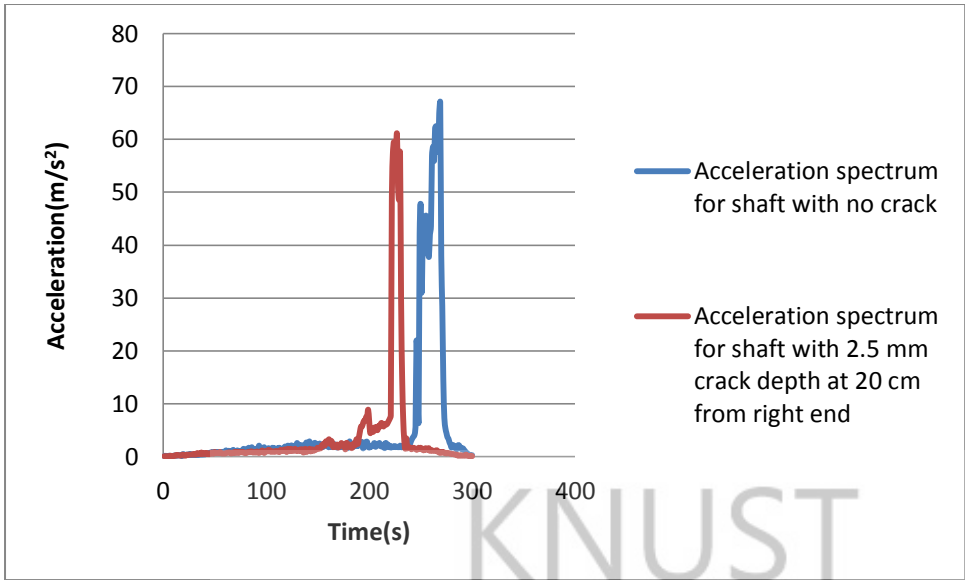


Figure 4. 21 Comparison between the acceleration spectrum of an intact shaft and a shaft with 2.5 mm crack depth at 20 cm from right end

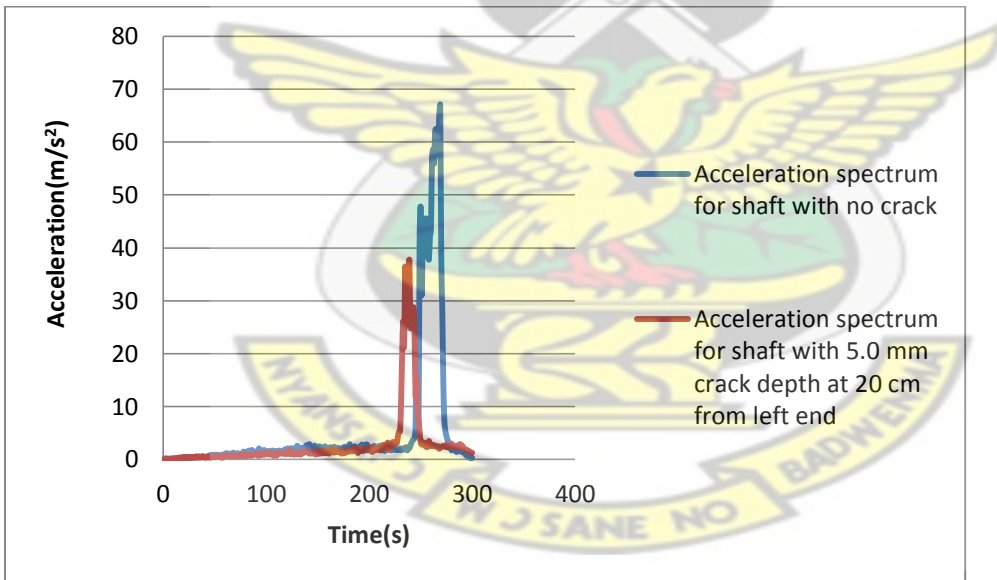


Figure 4. 22 Comparison between the acceleration spectrum of an intact shaft and a shaft with 5.0 mm crack depth at 20 cm from left end

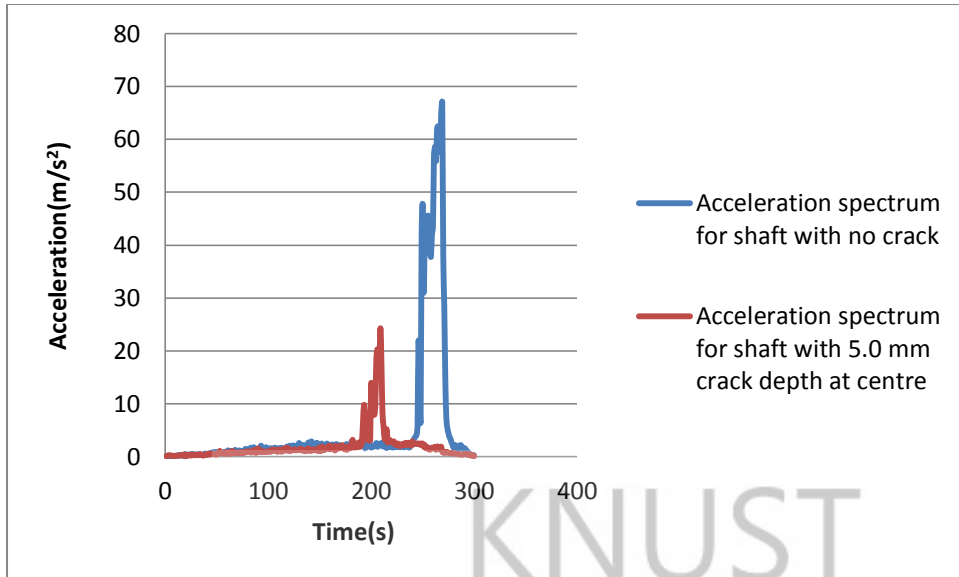


Figure 4. 23 Comparison between the acceleration spectrum of an intact shaft and a shaft with 5.0 mm crack depth at centre

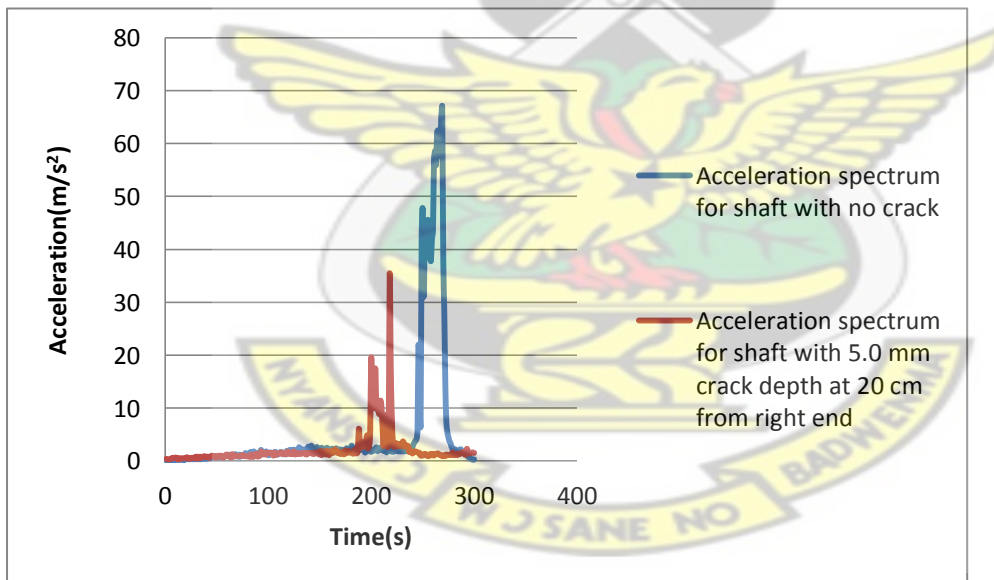


Figure 4. 24 Comparison between the acceleration spectrum of an intact shaft and a shaft with 5.0 mm crack depth at 20 cm from right end

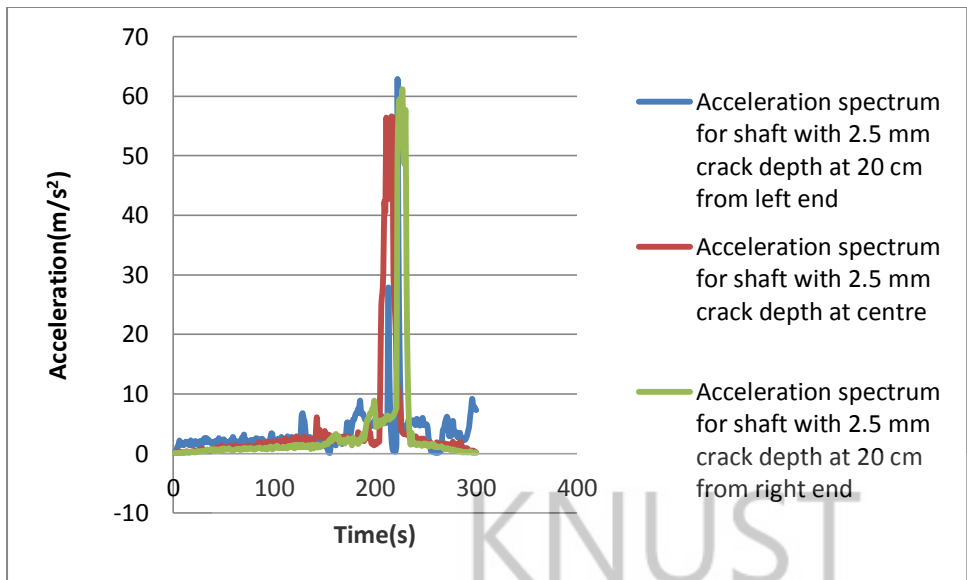


Figure 4. 25 Comparison between the acceleration spectrums of shafts with 2.5 mm crack depth at different positions (20cm, 36.8cm & 53.6cm).

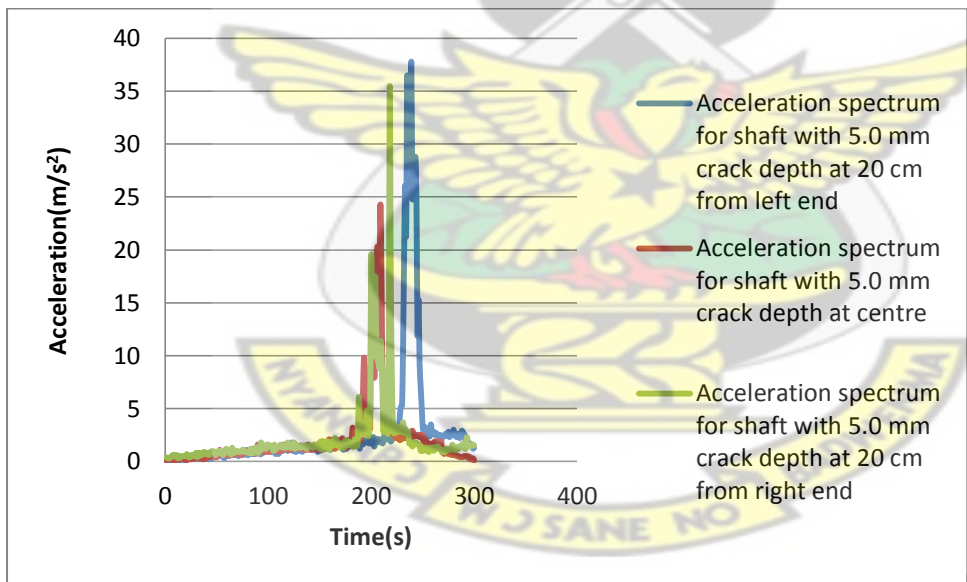


Figure 4. 26 Comparison between the acceleration spectrums of shafts with 5.0 mm crack depth at different positions (20cm, 36.8cm & 53.6cm).

From the acceleration spectrum, it is evident that the peak acceleration is maximum in the intact shaft. There is a reduction in the resonant value with the introduction of a crack. If the

crack width is held constant, there is a correlation between the crack depth and the peak acceleration. The deeper the crack, the lower the acceleration required for resonance to occur.

Cracks of the same depth but placed at different locations on the shaft had different peak accelerations, those at the middle had a relatively lower peak values as compared to those closer to the supports (trunnion blocks).

4.2.2 Effect of crack depth and position on the natural frequency (whirling speed) of a shaft

The frequency at which resonance occurred which corresponds to the natural frequency of transverse vibration or the whirling speed of the shaft is presented in Table 4.2.

Table 4. 2 Experimental frequency results for different crack depths and positions

Crack position (mm)	Crack depth (mm)	Frequency (rpm)
200	0	1165
	2.5	1164
	5.0	1161
	7.5	1159
368	0	1165
	2.5	1161
	5.0	1158
	7.5	1156
536	0	1165
	2.5	1163
	5.0	1160
	7.5	1158

From the above results, it is evident that the presence of a crack reduces the fundamental frequency (whirling speed) of the shaft. Increases in crack depth result in the lowering of the natural frequency. From the experiment, it was evident that the position of the crack has a telling influence on the frequency. The decrease of frequency for cracks situated at the middle of the shaft was higher as compared to those at the ends.

An analytical approach employing Dunkerley's empirical method was also used to compute the natural frequency. Matlab codes (Appendix B) were also developed to aid in the computation of the shaft's natural frequency in hertz as well as the whirling speed in *revolution per minute (rpm)*. The program also gave results of the deflection caused by the mass of the shaft as well as the external loads carried by the shaft relative to the crack depth. In writing the program, the width of the crack which was 1 mm remained constant with the crack depth varied. The results are indicated in table below.

Table 4. 3 Analytical Frequency results

Crack position (mm)	Crack depth (mm)	Frequency (Hz)	Frequency (rpm)
100	0	19.5292	1171.75
	2.5	19.5273	1171.64
	5.0	19.5206	1171.24
	7.5	19.5128	1170.77
200	0	19.5292	1171.75
	2.5	19.5223	1171.34
	5.0	19.5169	1171.01
	7.5	19.5037	1170.22
368	0	19.5292	1171.75

	2.5	19.5144	1170.86
	5.0	19.5088	1170.53
	7.5	19.4887	1169.32
536	0	19.5292	1171.52
	2.5	19.5199	1171.19
	5.0	19.5137	1170.82
	7.5	19.5008	1170.05
636	0	19.5292	1171.75
	2.5	19.5212	1171.27
	5.0	19.5139	1170.83
	7.5	19.5025	1170.15

The Matlab program confirmed the results obtained experimentally with an error margin of 0.55%-1.03%.

A numerical approach using Solidworks (Ver.2014) was also used to compute the natural frequency in *hertz* (Hz). The results are indicated in table 4.4 below.

Table 4. 4 Numerical frequency and deformation scale results

Crack position (mm)	Crack depth (mm)	Frequency (Hz)	Frequency (rpm)	Deformation Scale
100	0	19.657	1179.42	0.0372811
	2.5	19.654	1179.24	0.0372795
	5.0	19.652	1179.12	0.0372691
	7.5	19.612	1176.72	0.0372257
200	0	19.657	1179.42	0.0372811

	2.5	19.650	1179.00	0.0372817
	5.0	19.613	1176.78	0.0372795
	7.5	19.496	1169.76	0.0372720
368	0	19.657	1179.42	0.0372811
	2.5	19.644	1176.78	0.0372859
	5.0	19.588	1176.8	0.0372997
	7.5	19.394	1169.76	0.0373489
536	0	19.657	1179.42	0.0372811
	2.5	19.648	1178.64	0.0372809
	5.0	19.644	1175.28	0.0372653
	7.5	19.654	1163.64	0.0372447
636	0	19.657	1179.42	0.0372811
	2.5	19.652	1178.88	0.0372778
	5.0	19.645	1178.64	0.0372716
	7.5	19.673	1179.24	0.0372449

The numerical frequency results also confirmed the experimental and analytical results.

Chapter 5: CONCLUSIONS and RECOMMENDATIONS

5.1 Conclusions

The main aim of the thesis was to investigate the effects of the depth and position of a crack on the static and dynamic behaviour of a shaft knowing that modal properties of a mechanical structure are directly influenced by its physical properties. There is no universally accepted algorithm for crack detection.

Torsional vibration experiment was carried on an intact and defective (cracked) shaft to see the effect of crack depth and position on the torsional rigidity. Graphs of torque against angle of twist were plotted for different crack depth and positions. The results were compared to that of an intact shaft and it was evident that the presence of a crack reduces its torsional rigidity. Increasing the depth of the crack reduced its rigidity further. For the same crack depth, the effect was more severe at the centre as compared to those closer to the ends.

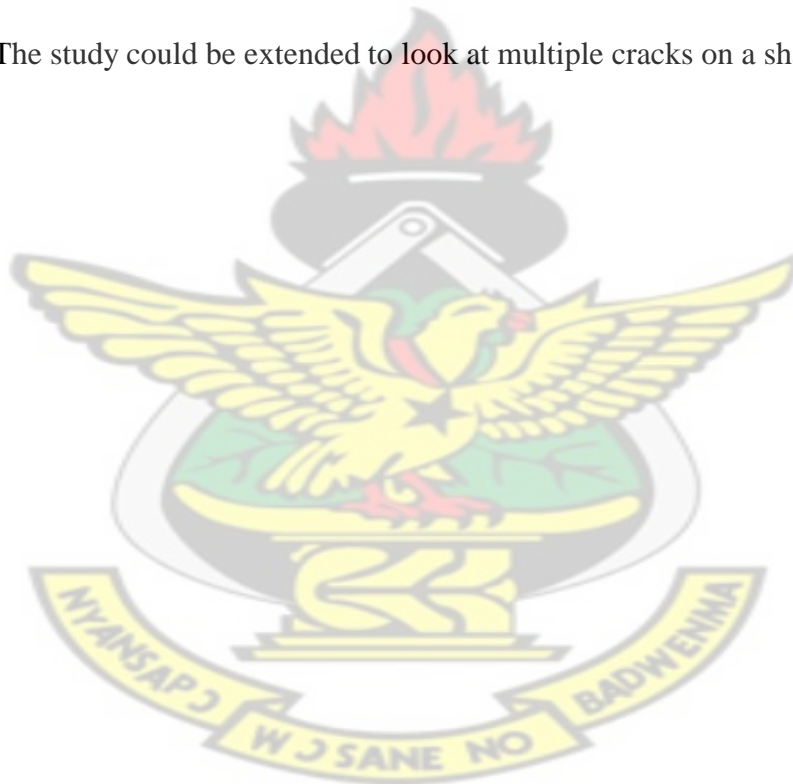
Transverse vibration experiment was also carried out to see the effect of crack depth and position on the fundamental natural frequency (whirling speed) and the acceleration of a shaft. The natural frequency and peak acceleration decreased in the defective shafts. It is safe to conclude that the critical speed decreases with the increase in crack. It was also observed that for the same crack depth, the crack at the middle position had the greatest reduction in natural frequency and acceleration. A Matlab program was developed to compute the natural frequency and the static deflection of the shaft. The small error differences (0.55%–1.03%) between experimental studies and the Matlab program demonstrated the consistency of the proposed method in the crack identification of a shaft. A numerical study was carried out using Solidworks and it confirmed the experimental and analytical approach.

From the results it can be deduced that, the presence of a crack reduces a cracks natural frequency and the severity is highest when the crack is located at the middle. Also, the analytical results were much closer to the experimental as compared to the numerical.

5.2 Recommendations

The results of this study do not provide a unique signature of crack therefore;

1. Further investigation is needed to develop models for shaft crack detection.
2. Further investigation is needed to distinguish crack signatures from other defects such as unbalance, looseness and misalignment.
3. The study could be extended to look at multiple cracks on a shaft.



REFERENCES

- Adewusi, S. A. and Al-Bedoor, B. O., 2002, "Detection of Propagating Cracks in Rotors Using Neural Networks," American Society of Mechanical Engineers, Pressure Vessels and Piping Division, Vancouver, Canada Vol. 447, 71-78.
- Allen, J. W. and Bohanick, J. S., 1990, "Cracked Shaft Diagnosis and Detection on Reactor Recirculation Pumps at Grand Gulf Nuclear Station," in International Exhibition and Conference for the Power Generation Industries - Power-Gen, May-June, Houston, TX Vol. 5-6, 1021- 1034.
- Bachschnid, N., Pennacchi, P., Tanzi, E., and Audebert, S., 2000a, "Identification of Transverse Cracks in Rotors Systems," in Proceedings of the 8th International Symposium on Rotating Machinery (ISROMAC-8), Honolulu, Hawaii, 26-30 March, 1-11.
- Bachschnid, N., Pennacchi, P., Tanzi, E., and Vania, A., 2000b, "Identification of Transverse Crack Position and Depth in Rotor Systems," *Meccanica*, Vol. 35, No. 6, 563-582.
- Baruh, H. and Ratan, S., 1993, "Damage Detection in Flexible Structures," *Journal of Sound and Vibration*, Vol. 166, 21-30.
- Bently, D. E. and Muszynska, A., 1986a, "Early Detection of Shaft Cracks on Fluid-Handling Machines," in Proceedings of the ASME International Symposium on Fluid Machinery Trouble Shooting, 1986 Winter Annual Meeting, Anaheim, CA, 7-12 December, ASME, Fluids
- Bently, D. E. and Muszynska, A., 1986b, "Detection of Rotor Cracks," in Proceedings of Texas A&M University 15th Turbomachinery Symposium and Short Courses, Corpus Christi, TX, November, 129-139.
- Bloch, H. P., 1997, *Machinery Failure Analysis and Troubleshooting*, 3rd Ed., Gulf Publishing, Houston, TX.
- Brandon, J., 2000, "Non-Linear Vibration of Cracked Structures: Perspectives and Horizons," *Shock and Vibration Digest*, Vol. 32, No. 4, 273-280.
- Brook, W. R. and Miller, W. H., 1991, "Crack Detection Method for Shaft at Rest," US Patent No. 5,068,800.
- Brose, W. R. and Jirinec, M. J., 1992, "East River No. 7 HP Rotor Crack Growth Analysis," in Proceedings of the American Power Conference, Illinois Institute of Technology, Chicago, IL, Vol. 54, Pt 2, 1326-1331.
- Carlson, G. J., Imam, I., Azzaro, S. H., and Scheibel, J. R., 1988, "Expert System for On-Line Rotor Crack Monitoring and Diagnostic System," in Proceedings of Computer Engineering, ASME, New York, 361-366.

Chan, R. K. C. and Lai, T. C., 1995, "Digital Simulation of a Rotating Shaft with a Transverse Crack," *Applied Mathematical Modelling*, Vol. 19, No. 7, 411-420.

Collins, K. R., Plaut, R. H., and Wauer, J., 1991, "Detection of Cracks in Rotating Timoshenko Beams Using Axial Impulses," *Journal of Vibration and Acoustics, Transactions of the ASME*, Vol. 113, 74-78.

Dimarogonas, A. D. and Papadopoulos, C. A., 1988, "Crack Detection in Turbine Rotors," in *Proceedings of 2nd International Symposium on Transport Phenomena Dynamics and Design of Rotating Machinery*, Honolulu, Hawaii, April 3-6, 286-298.

Dimarogonas, A. D. and Papadopoulos, C. A., 1992, "Coupled Vibrations of Cracked Shafts," *Journal of Vibration and Acoustics*, Vol. 114, No. 4, 461-467.

Dimarogonas, A. D., 1996, "Vibration of Cracked Structures: A State of the Art Review," *Engineering Fracture Mechanics*, Vol. 55, 831-857.

Dirr, B. O. and Schmalhorst, B. K., 1988, "Crack Depth Analysis of a Rotating Shaft by Vibration Measurement," *Journal of Vibration and Acoustics, Transactions of the ASME*, Vol. 110, No. 2, 158-164.

Dorfman, L. S. and Trubelja, M., 1999, "Torsional Monitoring of Turbine Generators for Incipient Failure Detection," in *Proceedings of 6th Steam Turbine/Generator Workshop*, St. Louis, MI, EPRI Report.

eFunda, Inc. "Carbon Steel aisi 1020." eFunda. 2014. http://www.efunda.com/materials/alloys/carbon_steels/show_carbon.cfm?id=aisi_1020&prop=all&page_title=aisi%201020 (accessed April 14, 2014).

Eisenmann, R. C., 2000, *Machinery Malfunction: Diagnosis and Correction*, Prentice Hall, Englewood Cliffs, NJ.

Feldman, M. and Seibold, S., 1998, "Damage Diagnosis of Rotors: Application of Hilbert Transform and Multi-Hypothesis Testing," *Reports of the Institut für Techno- und Wirtschaftsmathematik (ITWM)*, No. 2., 1-23.

Franklin, W., Bently, D. E., Goldman, P., and Muszynska, A., 1997, "Early Cracked Shaft Detection in Pumps Using Rotor Lateral Vibration Analysis," in *Pumping Machinery*, ASME Fluids Division Summer Meeting, Vancouver, Canada, Vol. 11, 8 pp.

Fuchs, H. O. and Stephens, R. I., 2000, *Metal Fatigue in Engineering*, 2nd Ed., Wiley, New York.

Gandy, D. and Viswanathan, V., 2001, "Repair Solutions for Steam and Gas Turbines," *Power Engineering*, Vol. 105, No. 3, 42-44.

Gasch, R. and Liao, M., 1996, "Process for the Early Detection of a Crack in a Rotating Shaft," US Patent No. 5,533,400.

Gasch, R., 1993, "A Survey of the Dynamic Behavior of a Simple Rotating Shaft with a Transverse Crack," *Journal of Sound and Vibration*, Vol.160, No. 2, 313-332.

Giridhar Sabnavis, R. Gordon Kirk, Mary Kasarda and Dane Quinn. "Cracked Shaft Detection and Diagnostics: A Literature Review." *The Shock and Vibration Digest*, 2004: 287-296.

Goldman, P. and Muszynska, A., 1992, "Torsional Vibration Measurements Help in Shaft Crack Diagnosis," *Orbit*, Vol. 13, No. 4, 5-7.

Goldman, P., Bently, D. E., and Muszynska, A., 1996, "Modal Diagnostics of Rotors with Cracks," in *IMEchE Symposium on Nonlinear Dynamics and Control*, Atlanta, GA, Vol. 91, 185-190.

Goldman, P., Muszynska, A., Bently, D. E., Dayton, K. P., and Garcin, M., 1999, "Application of Perturbation Methodology and Directional Filtering for Early Rotor Crack Detection," in *ASME International Gas Turbine and Aeroengine Congress and Exhibition (IGTI 1999)*, Indianapolis, IN, Paper No. 99-GT-225.

Gounaris, G. D. and Papadopoulos, C. A., 2002, "Crack Identification in Rotating Shafts by Coupled Response Measurements," *Engineering Fracture Mechanics*, Vol. 69, 339-352

Green, I. and Casey, C., 2003, "Crack Detection in a Rotor Dynamic System by Vibration Monitoring – Part I: Analysis," in *IGTI 2003*, Atlanta, GA, Paper No. GT2003-38659.

Guang, M. and Gasch, R., 1993, "Stability and Stability Degree of a Cracked Flexible Rotor Supported on Journal Bearings," in *Vibration of Rotating Systems*, ASME, Design Engineering Division, Albuquerque, USA, Vol. 60, 315-323.

Guo, D., Chu, F., and He, Y., 2003, "Vibration Analysis of Rotor with Transverse Surface Cracks," in *IGTI 2003*, Atlanta, GA, Paper No. GT2003-38041.

Hamidi, L., Piaud, J.-B., and Massoud, M., 1992, "A Study of Crack Influence on the Modal Characteristics of Rotors," in *International Conference on Vibrations in Rotating Machinery (ImechE)*, Bath, UK, No. C432/066, 283-288.

He, Y., Chu, F., Guo, D., and Zhong, B., 2001, "Study on Genetic Algorithms Based Rotor Crack Detection for Rotating Machine," *Chinese Journal of Mechanical Engineering*, Vol. 37, No. 10, 69-74.

Herbert, R. G., 1987, "Turbine-Alternator Run-Down Vibration Analysis: Automated Crack Detection," *ASME Design Engineering Division Publication*, Vol. 2, No. 2, 631-636.

Ichimonji, M., Kazao, Y., Watanabe, S., and Nonaka, S., 1994, "Dynamics of a Rotor System with a Slant Crack Under Torsional Vibration," in *Non-Linear and Stochastic Dynamics*, American Society of Mechanical Engineers, Applied Mechanics Division, Chicago, IL, Vol. 192, 81-90.

Imam, I., Azzaro, S. H., and Bankert, R. J., 1993, "System and Method for Detecting the Occurrence, Location and Depth of Cracks in Turbine - Generator Rotors," US Patent No. 5,258,923.

Imam, I., Azzaro, S. H., Bankert, R. J., and Scheibel, J., 1989, "Development of an On-Line Rotor Crack Detection and Monitoring System," *Journal of Vibration and Acoustics, Transactions of the ASME*, Vol.111, No. 3, 241-250.

Ishida, Y., Hirokawa, K., and Hirose, M., 1995, "Vibrations of a Cracked Rotor: 3/2-Order Super-Subharmonic and One Half-Order Sub-harmonic Resonances," in *Proceedings of 15th Biennial Conference on Mechanical Vibration and Noise, Boston, MA, American Society of Mechanical Engineers, Design Engineering Division*, Vol. 84, No. 3, Pt A/1, 605-612.

Ishida, Y., Inoue, T., and Nishimura, K., 2001, "Detection of a Rotor Crack by a Periodic Excitation," in *International Symposium on Stability Control of Rotating Machinery (ISCORMA 2001)*, Minden, NV, 1004-1011.

Iwatsubo, T., Arii, S., and Oks, A., 1992, "Detection of a Transverse Crack in a Rotor Shaft by Adding External Force," in *International Conference on Vibrations in Rotating Machinery (ImechE)*, Bath, UK, No. C432/093, 275-282.

Jenkins, L. S., 1985, "Cracked Shaft Detection on Large Vertical Nuclear Reactor Coolant Pump," *NASA Conference Publication 2409*, 253-265.

Kavarana, F. H. and Kirk, R. G., 1995, "Cracked Shaft Detection Using the Unbalance Excitation Technique," in *ASME DE*, Vol. 84-2, Vol. 3, Pt B, 1001-1007.

Kowal, M. G. and O'Brien, J. T. Jr., 1989, "Monitoring for Shaft Cracks on Reactor Recirculation Pumps," *Sound and Vibration*, Vol. 23, No. 5, 12-17.

Lazzeri, L., Cecconi, S., Faravelli, M., Scala, M., and Tolle, E., 1992, "Second Harmonic Vibration Monitoring of a Cracked Shaft in a Turbo-Generator," in *Proceedings of the American Power Conference, Chicago, IL*, Vol. 54, Pt 2, 1337-1342.

Lee, C.-W. and Kwon, K.-S., 2000, "Crack Detection in Rotating Machinery by Modal Testing," in *International Conference on Vibrations in Rotating Machinery (ImechE)*, Nottingham, UK, Paper No. C576/ 031/2000, 535.

Lees, A. W. and Friswell, M. I., 1999, "Crack Detection in Asymmetric Rotors," in *International Conference on Damage Assessment of Structures, DAMAS 99, Dublin, Ireland*, June, 246-255.

Lees, A. W., 2000, "Fault Diagnosis in Rotating Machinery," in *Proceedings of the International Modal Analysis Conference (IMAC)*, San Antonio, TX, Vol. 1, 313-319.

Leyzerovich, A., 1997, *Large Power Steam Turbines, Vols 1 and 2*, Pennwell, Tulsa, OK.

Liao, M. and Gasch, R., 1992, "Crack Detection in Rotating Shafts – An Experimental Study," in International Conference on Vibrations in Rotating Machinery (ImechE), Bath, UK, Paper No. C432/106, 289-295.

Maynard, K. P., Trethewey, M. W., and Groover, C., 2001, "Application of Torsional Vibration Measurement to Shaft Crack Monitoring in Power Plants," in Proceedings of the 55th Meeting of the Society for Machinery Failure Prevention Technology, Virginia Beach, VA, April 2-5.

Meng G. and Hahn, E. J., 1994, "Dynamic Response of a Cracked Rotor with Some Comments on Crack Detection," ASME, The Hague, Netherlands, Paper No. 94-GT-029, 1-10.

Miller, W. H. and Brook, W. R., 1990, "Shaft Crack Detection Method," US Patent No. 4,975,855.

Miller, W. H. and Brook, W. R., 1992, "Crack Detection Method for Operating Shaft," US Patent No. 5,159,563.

Mohiuddin, M. A. and Khulief, Y. A., 2002, "Dynamic Response Analysis of Rotor-Bearing Systems With Cracked Shaft," Journal of Mechanical Design, Transactions of the ASME, Vol. 124, No. 4, 690-696.

Munoz, R. Q., Ramirez, J., Antonio, S., and Kubiak, J. S., 1997, "Rotor Modal Analysis for a Rotor Crack Detection," in Proceedings of the International Modal Analysis Conference (IMAC), Bethel, CT, Vol. 1, 877-879.

Muszynska, A., 1989, "Misalignment and Shaft Crack-Related Phase Relationships for 1X and 2X Vibration Components of Rotor Responses," Orbit, Vol. 10, No. 2, 4-8.

Muszynska, A., Goldman, P., and Bently, D. E., 1992, "Torsional/Lateral Vibration Cross-Coupled Responses Due to Shaft Anisotropy: A New Tool in Shaft Crack Detection," in International Conference on Vibrations in Rotating Machinery (ImechE), Bath, UK, Paper No. C432/090, 257-262.

Ostachowicz, W. M. and Krawczuk, M., 1992, "Coupled Torsional and Bending Vibrations of a Rotor with an Open Crack," Archive of Applied Mechanics, Vol. 62, 191-201.

Papadopoulos, C. A. and Dimarogonas, A. D., 1989, "Coupled Vibration of Cracked Shafts," ASME, Design Engineering Division, Vol. 18, No. 2, 7-12.

Papadopoulos, C. A. and Dimarogonas, A. D., 1990, "Diagnosis of Edge Cracks in Rotating Shafts," in EPRI, 4th Incipient Failure Detection Conference, Predictive Maintenance for the 90s, Philadelphia, PA, October 15-17, 1-26.

Park, R.-W., 1996, "Crack Detection, Localization and Estimation of the Intensity in a Turbo Rotor," ASME, Jakarta, Indonesia, Paper No. 96-TA-031, 1-7.

- Plaut, R. H., Andruet, R. H., and Suherman, S., 1994, "Behavior of a Cracked Rotating Shaft During Passage Through a Critical Speed," *Journal of Sound and Vibration*, Vol. 173, No. 5, 577-589.
- Prabhakar, S., Sekhar, A. S., and Mohanty, A. R., 2001, "Detection and Monitoring of Cracks Using Mechanical Impedance of Rotor-Bearing System," *Journal of the Acoustical Society of America*, Vol. 110, No. 5, 2351-2359.
- Prabhu, B. S. and Sekhar, A. S., 1995, "Severity Estimation of Cracked Shaft Vibrations Within Fluid Film Bearings," *Tribology Transactions*, Vol. 38, No. 3, 583-588.
- Rajab, M. D. and Al-Sabeeh, A., 1991, "Vibrational Characteristics of Cracked Shafts," *Journal of Sound and Vibration*, Vol. 147, No. 3, 465-473.
- Ratan, S., Baruh, H., and Rodriguez, J., 1996, "On-Line Identification and Location of Rotor Cracks," *Journal of Sound and Vibration*, Vol. 194, No. 1, 67-82.
- Rieger, N. and El-Shafei, A., 2003, "Automated Diagnostics of Rotating Machinery," in *IGTI 2003*, Atlanta, GA, Paper No. GT2003-38453.
- Roberts, S. and Brandon, J. A., 2003, "Nonlinear Signatures in the Transient Dynamics of Turbo-Machinery," *Key Engineering Materials*, Vol. 245-246, 279-286.
- Rosard, D. D., Reid, S. R., and Blades, J. C., 1994, "Optimizing Maintenance Intervals Using a Turbine Rotor Crack Monitoring Program," *ASME*, Phoenix, AZ, 94-JPGC-PWR-5617, 1-8.
- Saavedra, P. N. and Cuitino, L. A., 2002, "Vibration Analysis of Rotor for Crack Identification," *Journal of Vibration and Control*, Vol. 8, No. 1, 51-67.
- Sanderson, A. F. P., 1992, "The Vibration Behavior of a Large Steam Turbine Generator During Crack Propagation Through the Generator Rotor," in *International Conference on Vibrations in Rotating Machinery (ImechE)*, Bath, UK, Paper No. C432/102, 263-273.
- Seibold, S. and Weinert, K., 1996, "Time Domain Method for the Localization of Cracks in Rotors," *Journal of Sound and Vibration*, Vol. 195, No. 1, 57-73
- Seibold, S., Fritzen, C.-P., and Wagner, D., 1996, "Employing Identification Procedures for the Detection of Cracks in Rotors," *International Journal of Analytical and Experimental Modal Analysis*, Vol. 11, No. 3-4, 204-215.
- Sekhar, A. S. and Prabhu, B. S., 1998, "Condition Monitoring of Cracked Rotors Through Transient Response," *Mechanism and Machine Theory*, Vol. 33, No. 8, 1167-1175.
- Sekhar, A. S., 1999, "Conditioning Monitoring of a Rotor System Having a Slant Crack in the Shaft," *Noise and Vibration Worldwide*, Vol. 30, No. 3, 23-31.
- Sekhar, A. S., 2000, "Detection and Monitoring of Cracks in Rotors Through Q Factors," *Proceedings of the Institution of Mechanical Engineers, Part C*, Vol. 214, No. 7, 949-954.

- Sekhar, A. S., 2004, "Detection and Monitoring of Cracks in a Coast-Down Rotor Supported on Fluid Film Bearings," *Tribology International*, Vol. 37, No. 3, 279-287.
- Shiohata, K., Satoh, K., Ohmori, M., Kikuchi, K., and Kaneko, R., 1987, "Method of and Apparatus for Detecting Crack Condition," US Patent No. 4,635,210.
- Soeffker, D., Bajkowski, J., and Mueller, P. C., 1993a, "Crack Detection in Turbo Rotors Vibrational Analysis and Fault Detection," *Vibrations of Rotating Systems*, Vol. 60, 277-286.
- Soeffker, D., Bajkowski, J., and Mueller, P. C., 1993b, "Detection of Cracks in Turbo Rotors – A New Observer Based Method," *Journal of Dynamic Systems, Measurement and Control, Transactions of the ASME*, Vol. 115, No. 3, 518-524.
- Subbiah, R., Montgomery, J., and Banks, R. L., 2002, "Studies on Rotor Cracks Due to Bending and Torsional Effects," in *Proceedings of 6th International Conference on Rotor Dynamics (IFTToMM)*, Sydney, Australia, 343-349.
- Sundermeyer, J. N. and Weaver, R. L., 1995, "On Crack Identification and Characterization in a Beam by Non-Linear Vibration Analysis," *Journal of Sound and Vibration*, Vol. 183, No. 5, 857-871.
- Thibault, S. E., Miller, W. H., Brook, W. R., Mannix, T. P., 1996, "Multiple Axis Transducer Mounting Collar," US Patent No. 5,520,061.
- Torres, M. R., 1996, "On-Line Shaft Crack Detector," US Patent No. 5,479,824.
- Tsai, T. C. and Wang, Y. Z., 1996, "Vibration Analysis and Diagnosis of a Cracked Shaft," *Journal of Sound and Vibration*, Vol. 192, No. 3, 607-620.
- Varé, C. and Andrieux, S., 2001, "Cracked Beam Section Model Applied to Turbine Rotors," in *International Symposium on Stability Control of Rotating Machinery (ISCORMA 2001)*, Minden, NV, 4002-4011.
- Wauer, J., 1990, "On the Dynamics of Cracked Rotors: A Literature Survey," *Applied Mechanics Reviews*, Vol. 43, No. 1, 13-17.
- Werner, F., 1993, "The Ratio of 2X to 1X Vibration – A Shaft Crack Detection Myth," *Orbit*, Vol. 14, No. 3, 11.
- Yang, W.-X., Qu, L.-S., and Jiang, J.-S., 2001, "Study of the Diagnostic Features of a Rotor with a Transverse Crack," *Insight, Non-Destructive Testing and Condition Monitoring*, Vol. 43, No. 8, 537-545.
- Yen, H.-Y. and Herman Shen, M.-H., 1997, "The Effects of Fatigue Cracks on Free Torsional Vibration of Shafts," in *IGTI 1997*, Paper No. 97- GT-249, 8 pp.
- Zakhezin, A. M. and Malysheva, T. V., 2001, "Modal Analysis Rotor System for Diagnostics of the Fatigue Crack," in *Condition Monitoring Conference 2001*, St Catherine's College, Oxford, UK, June 25-27.

Zhao, M. and Luo, Z. H., 1989, "Convenient Method for Diagnosis of Shafting Crack," ASME Design Engineering Division, Vol. 18, No. 1, 29-33.

Zhao, M. and Luo, Z. H., 1992, "An Expert System of Crack Monitoring and Diagnosing for Rotating Machines," in Proceedings of Conference on Rotating Machine Dynamics, Venice, Italy, 84-91.

Zou, J., Chen, J., Niu, J. C., and Geng, Z. M., 2003, "Application of the Wigner-Ville Distribution to Identification of a Cracked Rotor," Proceedings of the IMechE, Part C, Journal of Mechanical Engineering Science, Vol. 217, No. 5, 551-556.

Zou, J., Chen, J., Pu, Y. P., and Zhong, P., 2002, "On the Wavelet Time-Frequency Analysis Algorithm in Identification of a Cracked Rotor," Journal of Strain Analysis for Engineering Design, Vol. 37, No. 3, 239-246.



APPENDIX A

Table A 1 Transverse vibration acceleration results

Time (s)	Acceleration spectrum for shaft with no crack	Acceleration spectrum for shaft with 2.5 mm crack depth at 20 cm from left end	Acceleration spectrum for shaft with 2.5 mm crack depth at centre	Acceleration spectrum for shaft with 2.5 mm crack depth at 20 cm from right end	Acceleration spectrum for shaft with 5.0 mm crack depth at 20 cm from left end	Acceleration spectrum for shaft with 5.0 mm crack depth at centre	Acceleration spectrum for shaft with 5.0 mm crack depth at 20 cm from right end
1	0.1	0.2	0.1	0.1	0.1	0.1	0.4
2	0.2	0.4	0.1	0.1	0.1	0.2	0.3
3	0.1	0.6	0.1	0.1	0.2	0.2	0.3
4	0.1	1.2	0.3	0.1	0.1	0.3	0.3
5	0.1	1.4	0.2	0.1	0.1	0.2	0.4
6	0.2	2.2	0.4	0.1	0.1	0.2	0.4
7	0.1	1.5	0.2	0.2	0.1	0.2	0.6
8	0.1	1.7	0.2	0.1	0.2	0.1	0.5
9	0.1	1.7	0.2	0.1	0.2	0.1	0.6
10	0.2	1.4	0.2	0.1	0.2	0.1	0.6
11	0.2	1.6	0.2	0.2	0.2	0.2	0.6
12	0.2	2	0.2	0.3	0.2	0.2	0.3
13	0.3	1.8	0.4	0.2	0.1	0.2	0.5
14	0.2	1.9	0.2	0.3	0.1	0.2	0.3
15	0.3	1.7	0.2	0.3	0.2	0.3	0.5
16	0.3	1.4	0.2	0.2	0.4	0.3	0.5
17	0.3	2.2	0.3	0.2	0.2	0.2	0.5
18	0.1	2	0.3	0.3	0.3	0.4	0.5
19	0.5	1.4	0.4	0.4	0.1	0.2	0.5
20	0.3	1.5	0.4	0.2	0.2	0.4	0.5
21	0.4	2	0.5	0.3	0.4	0.1	0.7
22	0.3	2.1	0.5	0.2	0.5	0.3	0.5
23	0.4	1.7	0.5	0.4	0.3	0.4	0.4
24	0.3	1.8	0.4	0.3	0.3	0.3	0.4
25	0.5	1.4	0.5	0.4	0.3	0.2	0.6
26	0.3	2.1	0.7	0.4	0.4	0.3	0.5
27	0.5	1.7	0.4	0.4	0.5	0.4	0.6
28	0.3	1.4	0.6	0.4	0.3	0.3	0.5
29	0.4	2.2	0.8	0.5	0.4	0.3	0.7
30	0.4	2.3	0.5	0.4	0.5	0.4	0.8
31	0.3	2.6	0.6	0.5	0.4	0.3	0.4
32	0.5	1.9	0.5	0.4	0.6	0.3	0.8

33	0.4	2.6	0.5	0.7	0.4	0.4	0.5
34	0.3	1.9	0.4	0.5	0.5	0.5	0.8
35	0.4	2.3	0.5	0.6	0.6	0.3	0.6
36	0.4	2	0.5	0.5	0.4	0.3	0.7
37	0.4	1.8	0.5	0.8	0.5	0.2	0.8
38	0.4	1.7	0.7	0.6	0.6	0.4	0.9
39	0.6	1.8	0.8	0.5	0.5	0.3	0.7
40	0.4	2	0.8	0.7	0.4	0.4	0.8
41	0.5	2	0.7	0.7	0.3	0.4	0.8
42	0.5	2.1	1	0.5	0.5	0.6	0.6
43	0.6	1.8	1	0.7	0.4	0.4	0.7
44	0.7	2.1	0.8	0.5	0.4	0.6	0.9
45	0.7	2.6	1	0.5	0.5	0.6	0.9
46	0.8	1.7	1	0.6	0.3	0.5	1
47	0.7	2.3	0.8	0.8	0.6	0.5	0.9
48	0.9	1.6	1.4	0.6	0.5	0.5	0.9
49	0.8	2.2	0.8	0.6	0.4	0.4	0.6
50	0.7	2.4	1	0.9	0.5	0.4	0.8
51	0.9	2.1	0.8	0.7	0.5	0.5	0.9
52	0.8	2	0.7	0.7	0.6	0.6	1
53	0.9	1.7	1	0.7	0.6	1.1	0.8
54	0.7	1.8	1	0.7	0.5	0.7	1
55	0.7	1.9	1	0.9	0.7	0.7	0.9
56	0.7	1.8	1.3	0.7	0.6	0.6	0.6
57	0.9	2.3	0.9	0.6	0.3	0.6	0.9
58	0.9	1.8	0.9	0.6	0.4	0.8	0.8
59	0.9	2.8	1.1	0.6	0.5	0.6	1.2
60	1	2.1	1.1	0.6	0.7	0.9	1
61	1.2	1.8	1.1	0.7	0.8	0.7	1.1
62	1	2.1	1.4	0.7	0.8	0.5	0.9
63	1.1	1.9	1.2	0.8	0.7	0.8	0.7
64	1.1	2	0.9	0.8	0.6	0.9	0.7
65	1	1.9	1.1	0.8	0.7	1.1	1.3
66	1	2.1	1.1	0.6	0.6	0.7	0.9
67	1.1	2.2	1.2	0.7	0.7	0.8	0.8
68	1.3	2.7	1.1	0.7	0.8	0.6	1
69	0.9	2.5	1.1	0.9	0.6	0.8	1
70	0.9	3.2	1.1	0.7	0.7	0.8	1
71	0.8	1.7	1.1	0.9	0.5	0.7	0.9
72	1.2	2.3	1	0.9	0.7	0.8	0.9
73	0.8	1.9	0.9	0.7	0.6	0.7	0.9
74	1	1.9	1.4	0.8	0.9	0.6	1
75	1	1.8	1.3	0.9	0.8	0.9	1.1
76	0.9	2	1.1	0.9	0.6	0.7	1.1

77	1.2	2.3	1	0.8	0.8	0.8	0.9
78	1.5	2	1.1	0.9	0.7	0.8	0.9
79	1.2	2.1	1.2	0.7	1.1	1	0.9
80	0.9	2.3	1.3	0.7	0.6	0.9	0.9
81	1.4	2	1.3	0.7	0.7	1	0.8
82	1.4	2.6	1.1	0.9	0.9	0.9	0.8
83	1.7	2.1	1.2	0.9	0.8	0.8	1.2
84	1.3	2.5	1.8	0.9	0.7	0.8	0.8
85	1.4	1.8	1.8	1	0.9	1.2	0.9
86	1.8	2	1.2	1	0.7	1.1	0.8
87	1.3	2.2	1.7	0.8	0.8	1.2	1.2
88	1.3	2.5	1.7	0.8	0.9	0.7	1.3
89	1.5	2	1	0.8	0.9	1.2	1.3
90	1.2	2.1	1.6	0.8	1.1	1.6	0.8
91	1.5	2	1.6	1	1.1	0.9	1.2
92	1	1.8	1.9	0.8	0.7	1	1
93	2.1	2	1.3	0.7	0.7	1.2	1.8
94	1.4	2	1.9	0.9	1.1	0.9	1.4
95	1.6	1.9	1.9	1	0.8	0.9	1.4
96	1.4	2.5	1.8	1.2	1.1	0.9	1.2
97	1.4	3.4	1.4	1	0.9	1	1.5
98	1.8	3.3	1.9	0.7	1.3	0.9	1.2
99	1.2	1.9	2	0.9	0.9	0.9	1.6
100	1.1	2.3	2	1	1.2	1	1.5
101	1.1	2.3	1.9	1.2	1.1	1	1.5
102	1.6	2.3	2.1	1	1	0.9	1.5
103	1.5	2.3	2	1.3	0.9	1.3	1.5
104	1.3	2.5	1.5	1	1.3	1.1	1.3
105	1.4	2.1	2	0.9	1	1.1	1
106	1.7	2	1.9	1	1	1.4	1.6
107	1.6	2.8	2.2	1	0.7	1.2	1.1
108	1.6	2.1	2.2	0.9	0.9	1.1	1.3
109	1.2	2.3	2.1	1	1	0.9	1.3
110	1.3	2	2.2	1.1	0.7	1.1	1.4
111	1.6	2.2	2.5	1	1	1.4	1.4
112	1.6	2.2	1.4	0.9	1.4	1	1.6
113	1.7	2.9	1.9	0.9	1.3	1	1.4
114	1.3	2.4	1.3	1.3	1.1	1	1.3
115	1.3	1.8	1.8	1.1	1.1	1.5	1.5
116	1.5	2.2	2.1	1.1	1.1	1.6	1.3
117	1.2	2.8	2.5	1.1	1.1	1.2	1.5
118	1.9	2.6	2.3	1.4	1.1	1.2	1.3
119	1.7	1.7	2.6	1.1	1	1.7	1.8
120	1.6	1.7	1.8	0.9	1.4	1.1	1.4

121	2.1	1.9	2.5	1.5	1.2	1.3	1.4
122	1.8	1.4	2.9	1.1	1.1	1.1	1.3
123	1.7	1.6	2.3	1.1	1.8	1.3	1.3
124	2.1	1.8	1.9	1.5	1	1.3	1.5
125	2.1	1.7	2.1	1.1	1.2	1.2	1.8
126	1.8	2.9	2.4	1.1	1	1.4	1.2
127	1.9	6.3	2.1	1.2	0.9	1.2	1.6
128	2	6.8	2.1	1.5	1.2	1.3	1.3
129	2.1	5.9	2.9	1.1	1.2	1.2	1.3
130	2.6	5.3	2.1	1.2	1	1.4	1.4
131	2.2	3.4	1.9	1.1	1.4	1.5	1.4
132	2.1	1.5	2.2	1.1	1.2	1.5	1.3
133	2.2	1.6	2.6	1.4	0.9	1.2	1.5
134	1.8	2.2	2.3	1.1	1.3	1.1	1.5
135	1.8	2.8	2.5	1.4	1.1	1.3	1.4
136	2.2	1.8	2.2	0.8	1.5	1.1	1.5
137	1.8	1.8	2.3	1	1.3	1.3	1.2
138	1.9	2.3	2.2	1.5	1.5	1.1	1.3
139	2.7	2.6	2.2	0.9	1.5	1.6	1.5
140	1.7	2	2.5	1.1	1.4	1.2	1.5
141	1.9	2.8	3.1	1.2	1.2	1.1	1.5
142	2.9	2	6.1	1.5	1.1	1.1	1.4
143	1.9	1.7	3.6	1	1.2	1.4	1.5
144	2.1	1.9	3.5	1.2	1.1	1.3	1.3
145	2.2	2.3	4	1.4	1.2	1.2	1.6
146	1.9	1.8	2.7	1.1	1.5	1.4	1.4
147	2.6	1.7	3.4	1.3	1.3	1.3	1.5
148	2.5	2.1	2.7	1.3	0.9	1.1	1.4
149	2.2	2	2.8	1.5	1.3	1.1	1.7
150	2	1.7	3.8	1.7	1	1.8	1.2
151	2.1	1.2	2.5	1.5	1.4	1.1	1.9
152	2.5	1	3.1	1.7	1.7	1.2	1.1
153	2	0.6	3.2	1.6	1.1	1.9	1.6
154	1.9	0.2	2.9	2.2	1.5	1.3	1.7
155	1.8	0.1	3.1	2	1.2	1.3	1.8
156	2.1	1.5	2.6	2.5	1.7	1.4	1.2
157	2.5	2	2.4	2.1	1.2	1.5	1.9
158	2.2	2.2	2.5	2.9	1.3	1.6	1.7
159	2.2	2	2.6	2.7	1.6	2.1	1.1
160	1.9	1.9	2.2	2.8	1.3	1.4	1.4
161	1.8	1.4	2.2	3.3	1.1	2	1.7
162	2.3	2.6	2.2	2.4	1.3	1.8	1.9
163	2.2	2.4	2.2	3	1.6	1.7	1.5
164	1.8	2	2.6	2.7	2	1.3	1.9

165	2.1	1.9	2.8	1.8	1.4	1.2	2.2
166	2.4	2.2	2.6	2.1	1.3	2.1	1.6
167	2.2	1.6	2	1.9	1.4	1.5	1.9
168	1.9	2	2.8	2.1	1.5	1.7	1.5
169	1.7	2.5	2.9	2.3	1.7	1.6	1.5
170	2.2	2.1	2.6	1.7	1.4	2	1.3
171	1.9	2.9	2.4	2.2	1.5	1.6	1.6
172	1.8	5.2	2.1	2.1	1.3	2.2	1.7
173	2.1	5.2	2.9	2.6	1.1	1.8	1.3
174	1.9	3.3	2.6	2.2	1.5	1.4	1.3
175	1.9	2.4	2.5	2	1.2	1.6	2
176	2.4	3.6	2.4	1.9	1.2	1.3	1.7
177	2	4.7	2.4	1.4	1.7	1.4	1.5
178	2	5.7	2.5	2.6	1.5	2	1.9
179	1.6	5.7	2.5	2.4	1.4	2	1.7
180	1.9	6.3	2.3	2	1.6	1.6	1.6
181	2.9	6.8	2.5	1.9	1.6	1.8	1.7
182	2.2	6.8	2.2	2.2	1.7	3.2	1.4
183	1.8	7.5	3.6	1.6	1.5	2.2	1.4
184	1.9	7.5	2.8	2	2	1.7	2.1
185	1.9	8.9	2.4	2.5	1.6	2.3	1.9
186	2.5	6.7	2.2	2.1	2.2	1.8	1.4
187	2.2	6.8	2.4	2.9	1.7	1.9	1.8
188	2	6.7	2.4	3.3	1.9	2.7	6.1
189	2.2	6.1	2.1	2.4	1.2	1.9	3.6
190	2.1	5.7	2.8	3.6	1.8	2.1	2.5
191	2.5	5.6	2.5	4.7	2	2.7	3.6
192	2.3	5.2	2.9	5.7	1.6	6.3	2.6
193	2.8	5	4.7	5.7	2	9.8	3.4
194	1.6	5	3.1	6.3	1.9	7.9	3.1
195	1.9	4.5	3.5	6.8	1.8	3.4	3.7
196	1.9	5.1	1.8	6.8	2	3.3	4.8
197	2.8	5	1.6	7.5	1.8	3.1	2.4
198	2.8	4.7	1.6	7.5	1.7	3.6	2.8
199	2	5.5	1.4	8.9	1.8	3.1	4.8
200	1.7	5.4	2	6.7	1.7	13.8	19.3
201	2	5.6	1.6	4.5	2	10.2	14.6
202	1.9	5	1.8	5.1	2.3	10.9	11.2
203	2	5.8	2.1	5	1.4	7.9	10.1
204	2.1	5.6	2	4.7	2.1	9.7	17.5
205	2.6	6.1	12.8	5.5	2.1	18.5	10.3
206	1.9	6.4	25	5.4	2.1	20.3	9.7
207	2	6	26.9	5.6	1.8	19.8	9.4
208	2.3	5.7	30.5	5	2.1	17.6	8.9

209	2.3	5.8	42.3	5.8	1.9	24.3	11.4
210	2.6	5.1	40.7	5.6	2	17.2	10.2
211	2	5.5	56.4	6.1	1.7	8.2	6.6
212	2	5.3	44.9	6.4	1.9	5.8	2.8
213	1.9	27.9	42.8	6	2.7	3.4	6.2
214	2.3	13.6	52	5.7	2.7	3.2	8.7
215	1.6	6.3	50.2	6.2	2.3	5.2	6.4
216	2.6	2.7	56.6	6.1	2.1	2.7	2.6
217	2.2	0.9	56.5	6.1	2.1	2.9	4.3
218	2.3	0.4	30.3	6.4	3.2	3.2	35.5
219	1.8	1.2	25.6	6.8	1.9	2.8	17.8
220	2.1	0.3	22.1	7.2	2	2.8	8.6
221	1.7	1.6	15.6	7.8	2.5	2.6	3.8
222	1.9	62.1	11.2	49.2	2.6	2.9	2.7
223	1.8	34.8	10.7	57.3	3.3	2.4	2.7
224	2	18.5	9.4	59.5	3	2.2	3.4
225	2	9.4	6.3	56.9	3.2	2.3	2.8
226	1.8	4.5	3.8	57.7	3	2.5	2.9
227	1.9	3.9	3.6	61	3.2	2.1	3.2
228	1.8	4.1	3.3	51.2	4.5	2	2.8
229	1.8	4.3	3.4	48.7	5.2	2.1	2.9
230	2.1	4	3.3	57.2	5.3	2.4	3.1
231	1.8	4.8	3.2	29.5	11	2.2	3.7
232	1.8	4.8	3.1	15.1	19.6	2.2	2.7
233	2.1	5.7	3.3	7.4	26.1	2.6	3.1
234	1.9	4.9	3	3.3	21.5	2.6	2.9
235	2.1	5.3	2.9	1.5	36.5	2.2	2.8
236	2.3	5.1	2.9	3.5	26.7	2.6	2.8
237	1.7	5.6	2.8	1.6	33.9	2.6	1.7
238	2.2	5.1	2.9	1.9	30.5	2.4	1.8
239	2.1	5.1	2.7	1.7	37.8	2.1	1.8
240	2.6	4.8	2.9	1.7	24.9	2.9	1.4
241	3.1	5.8	2.6	1.4	26.2	2.6	1.6
242	3.5	5.7	2.5	1.6	26.6	2.5	1.8
243	3.8	5.1	2.4	1.7	28.8	2.4	1.8
244	4.1	4.7	2.4	1.6	24.6	2.4	1.7
245	5.6	4.9	2.5	1.5	12.1	2.5	1.6
246	22	5.3	2.5	1.3	15.3	2.5	1.6
247	11.2	6	2.3	1.4	9.3	2.3	1.5
248	6.9	4.8	2.5	1.7	7.2	2.5	1
249	42.1	4.9	1.7	1.5	5.3	2.2	1.1
250	47.8	4.8	1.8	1.7	3.3	2.5	1
251	31	4.9	1.8	1.5	2.8	1.9	1.3
252	40.5	4.2	1.4	1.3	3.2	2.2	1.1

253	38.4	2.3	1.6	1.2	3.2	1.6	1.3
254	43	2	1.8	1.5	2.8	1.9	1
255	45.6	0.5	1.8	1.6	2.4	1.5	1
256	44.2	0.4	1.7	1.3	2.5	1.5	0.9
257	39.9	0.3	1.6	1.5	2.4	1.3	1.3
258	37.8	0.2	1.6	1.6	3.5	1.6	1.1
259	42	0.2	1.5	1.1	2.7	1.7	1.3
260	43.6	0.1	1.6	1.3	2.6	1.6	1.3
261	56.9	0.1	1.9	1.2	2.8	1.6	1
262	58.6	0.1	1.5	1.1	2.5	1.9	1.3
263	55.9	0.2	1.5	1.1	2.7	1.3	1.3
264	62.1	0.3	1.3	1.1	2.5	1.9	1.4
265	62.5	0.4	1.6	1.2	2.4	1.9	1.4
266	60.2	2.1	1.7	1.2	2.4	1.8	1.2
267	57.8	4	1.6	0.9	2.5	1.4	1.1
268	64.9	3.9	1.6	0.8	2	1.9	1.1
269	66.9	5.1	1.7	0.7	2.3	0.9	0.9
270	38	5.7	1.2	0.9	2.4	0.8	0.9
271	28.5	6.2	1.3	0.8	2.4	0.7	1.1
272	14.6	5.7	1.6	0.9	2.6	0.9	0.9
273	7.3	3	1.3	0.7	2.5	0.8	1.2
274	5.4	3.2	1.1	0.7	2.4	0.9	1.1
275	4.5	2.9	1.3	0.6	2.8	0.7	1.1
276	3.7	3.6	1.6	0.7	2.3	0.7	1.1
277	3.4	5.5	2	0.7	2.6	0.7	1.2
278	2.7	3.6	1.4	0.6	2.5	0.6	1.2
279	2.3	3.7	1.3	0.6	2.5	0.7	1.6
280	1.7	3.6	1.4	0.5	3	0.7	1.1
281	2.2	2.9	1.5	0.5	2.5	0.6	1.3
282	2.1	2.9	1.7	0.5	2.5	0.6	1.2
283	1.7	2.6	1.4	0.4	2.3	0.5	1.1
284	1.8	3.5	1.4	0.4	2.6	0.5	1.4
285	1.4	2.4	1.9	0.4	2.5	0.5	1.2
286	2.1	2.3	0.9	0.2	2.2	0.4	1.4
287	2.2	2.2	0.8	0.2	2.5	0.4	1.4
288	1.9	2.6	0.7	0.2	2.9	0.4	1.5
289	1.6	2.3	0.9	0.3	2.8	0.4	1.7
290	1.4	2.6	0.8	0.2	2.6	0.5	1.4
291	1.6	3.1	0.9	0.2	2.5	0.5	1.2
292	1.3	3.8	0.7	0.2	1.9	0.5	1.2
293	1.1	4.5	0.4	0.2	1.8	0.4	2.3
294	0.8	6.2	0.4	0.4	1.9	0.5	1.6
295	0.7	7.5	0.5	0.2	1.7	0.3	1.6
296	0.5	9.2	0.5	0.2	1.7	0.4	1.4

297	0.4	8	0.5	0.1	1.6	0.2	1.5
298	0.3	7.9	0.4	0.1	1.4	0.2	1.6
299	0.2	7.6	0.2	0.2	1.2	0.3	1.6
300	0.3	7.3	0.2	0.1	1.3	0.1	1.5

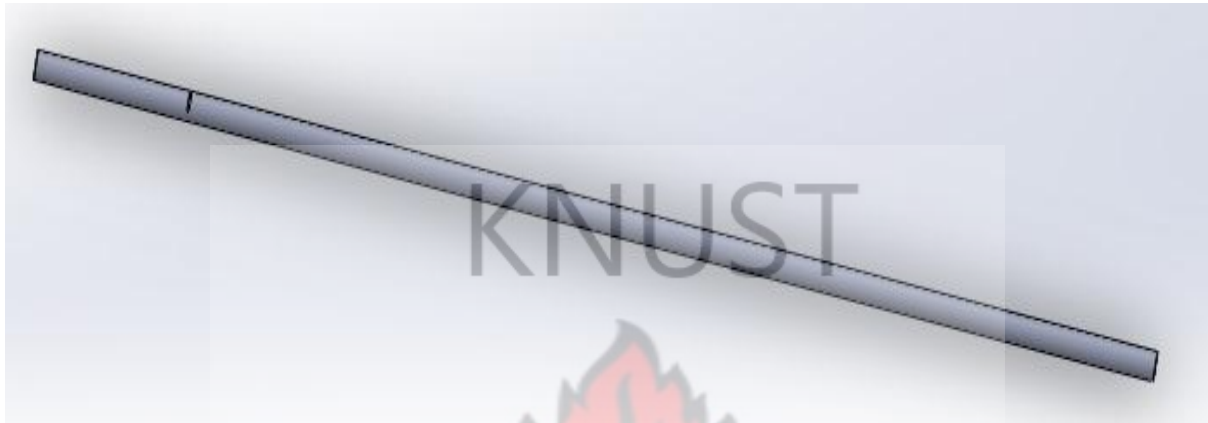


Figure A1 Modelled crack in Solidworks (100 mm from left end)



Figure A2 Modelled crack in Solidworks (200 mm from left end)



Figure A3 Modelled crack in Solidworks (at the centre of the shaft)



Figure A4 Modelled crack in Solidworks (536 mm from left end)



Figure A5 Modelled crack in Solidworks (636 mm from left end)

Model name: Rod
Study name: Frequency 3(-Default-)
Plotype: Frequency Amplitude1
Mode Shape: 1 Value = 19.657 Hz
Deformation scale: 0.0372811

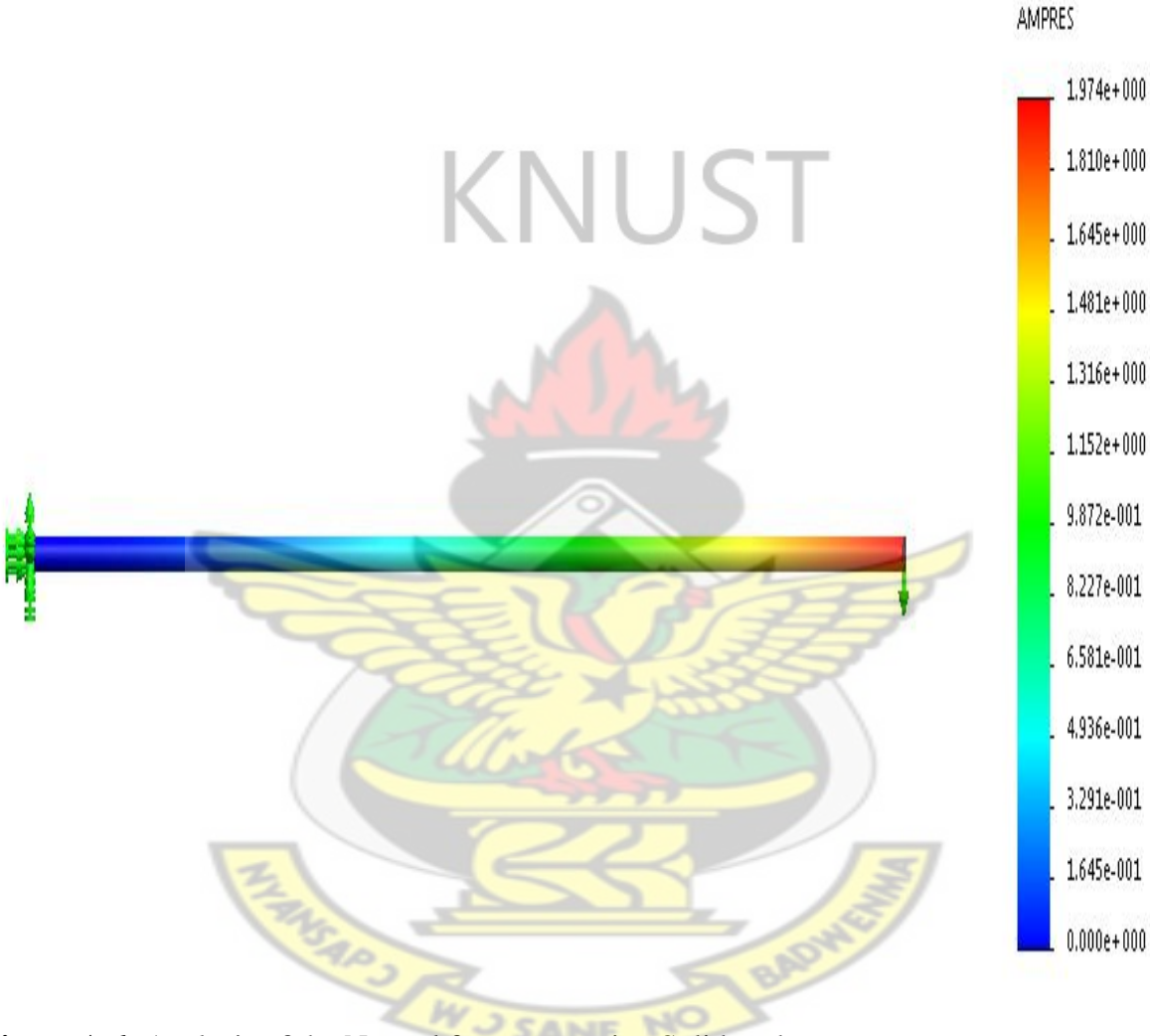


Figure A 6: Analysis of the Natural frequency using Solidworks

APPENDIX B

Matlab code for frequency analysis

```
m=1.03;
mmotor=3.8;
rho=7890;

r=0.0075;
ls=0.736
a=ls/2;
b=ls/2;
E=210*(10^9);
vol=pi()*(r^2)*ls
posm=0.368;
n=input('Enter number of portion, n: ');
massp=[];
deflscr=[];
dfreqhzc=[];
dspeedrpmc=[];
deflsc=0;
dfreqhzc=0;
l=[];
for i= 1:n
    i
    l(i)=input('portion length, li: ');
    if i==2
        crackw=input('crack width, crackw: ');
        crackd=input('crack depth crackd: ');
        theta=2*acosd((r-crackd)/r)
        alpha=theta*pi()/360
        smac=SMA-(0.25*(r^4)*(alpha+2*((sin(alpha))^3)*cos(alpha)-...
        sin(alpha)*cos(alpha)))
        areac=0.5*(r^2)*((theta*pi()/180)-sind(theta))
        volc=crackw*areac
        massc=rho*volc
        massp(i)=(l(i).*m/ls)-massc;
        dfreqhzc(i)=0.4985/(sqrt((deflscr(i)/1.27)))
        dspeedrpmc(i)=60*dfreqhzc(i)
    else
        massp(i)=l(i).*m/ls;
        deflscr(i)= (5*massp(i)*9.81*l(i)^4)/(384*E*SMA)
        dfreqhzc(i)=0.4985/(sqrt((deflscr(i)/1.27)))
```

```

    dspeedrpmc(i)=60*dfreqhzc(i)
end
deflsc=deflsc+deflscr(i)
dfreqhzx=dfreqhzx+(1/dfreqhzc(i))
end
if (l(1)+l(2))< a
    dfreqhzx = dfreqhzx- (1/dfreqhzc(3))
elseif (l(1)+0.5*l(2)) == a
    dfreqhzx = dfreqhzx- (1/dfreqhzc(2))
elseif l(1) > a
    dfreqhzx = dfreqhzx- (1/dfreqhzc(1))
end
mshaftc=m-massc;
dfreqhz=0.4985/(sqrt(deflm+(defls/1.27)))
dspeedrpm=60*dfreqhz
dfreqhzm=0.4985/(sqrt(deflm+(deflscr(3)/1.27)))
dfreqhzm=1/dfreqhzm
dfreqhzt=dfreqhzx+dfreqhzm;

```

